UCLouvain

epl

École polytechnique de Louvain

Bipolar DC microgrids: State of the art and solutions to voltage unbalance problem

Author: **Antoine KNOCKAERT**
Supervisor: **Emmanuel DE JAEGER**
Readers: **Marc BEKEMANS, Bruno DEHEZ, Eduardo VASQUEZ MAYEN**
Academic year 2022–2023
Master [120] in Electrical Engineering

Acknowledgements

I am indebted to my esteemed supervisor, Professor Emmanuel de Jaeger, and the invaluable guidance provided by PhD candidate Eduardo Vasquez Mayen and Professor Marc Bekemans. Their unwavering support throughout the year made the realization of this thesis possible.

I would like to express my heartfelt gratitude to Emmanuel de Jaeger, Eduardo Vasquez Mayen, Marc Bekemans and Bruno Dehez for accepting their roles as readers and jury members.

Special thanks go to Lund University generously granting me access to the Matlab license, which enabled me to conduct all simulations on my personal computer, significantly enhancing the efficiency of this crucial aspect of my thesis.

I extend my sincere appreciation to Stella, Frédéric, Noha, Laureline, Eduardo, and my father Olivier, whose meticulous proofreading provided invaluable feedback, enabling constant improvement in my work.

My deepest gratitude also goes to my family, Stella, Kajsa, Jarste, Noha, Laureline, Camille, Julia, Christophe, Emily, Justin and to my incredible exchange "Steve Aoki" group. Their good vibes and encouragement bolstered me during challenging times.

Finalement, j'aimerais tout particulièrement remercier mes sœurs, Chiara et Maïlys, auprès de qui chaque instant passé illumine mes journées. Vous êtes des personnes incroyables, et moi, ainsi que toutes les personnes que vous côtoyez, sommes extrêmement chanceux de vous avoir dans nos vies.

Abstract

This master's thesis investigates the problem of voltage unbalance, its consequences and its potential solutions in the context of bipolar DC microgrid. To address those questions, a state of the art is conducted to give a comprehensive overview of all existing solutions in the literature. Then, three devices are chosen based on suggested criteria, thoroughly designed and validated on small testbenches. Subsequently, simulations are conducted on a bigger testbench that represents better real-life scenarios. From the results of those simulations, it is concluded that the studied solutions provide good balancing capabilities and can maintain a bipolar DC microgrid stable. From those results, this work opens a discussion about the possible locations of those balancing devices within a grid. Finally, this thesis gives insight on the current state of standardization for bipolar DC electrical network.

Table of abreviations

AC	Alternating Current
CR	Current Redistributor
DC	Direct Current
DG	Distributed Generation
DCMG	DC Microgrid
EMC	ElectroMagnetic Compatibility
ESS	Energy storage system
IEC	International Electrotechnical Commission
IEEE	Institute of Electrical and Electronics Engineers
IGBT	Insulated Gate Bipolar Transistor
LCUR	Line Current Unbalance Rate
LVDC	Low Voltage Direct Current
LVUR	Line Voltage Unbalance Rate
MG	Microgrid
MOSFET	Metal-Oxyde-Semiconductor Field-Effect Transistor
NPC	Neutral Point Clamped
PID	Proportional Integral Derivative (Controler)
PV	PhotoVoltaic
SEPIC	Single Ended Primary Inductance Converter
VB	Voltage Balancer
VSC	Voltage Source Controller

Nomenclature

Θ	Duty cycle
e_i	Current error
e_v	Voltage error
f	Frequency
f_{sw}	Switching frequency
f_{BOI}	Bandwidth of the current control loop
f_{BOV}	Bandwidth of the voltage control loop
i_n	Negative wire's current
i_p	Positive wire's current
i_z	Neutral wire's current
s	Complex variable of the Laplace domain
P_{losses}	Power losses
T_{sw}	Switching period
V_n	Negative pole's voltage
V_p	Positive pole's voltage
V_{ref}	Reference voltage

Contents

List of Figures

List of Tables

Introduction

Background

The harmful effects of fossil fuels and greenhouse gas emissions are widely recognized nowadays [4]. While those emissions are produced by different sectors, a significant portion comes from electricity and heat production, reaching close to 42% of global emissions [5]. This has led to increased focus on developing carbon-free alternatives for generating power.

As a result, renewable energy sources have become more and more popular in the last decade, with installed capacity of wind and solar energy sources growing exponentially [6]. As much as they have advantages over their fossil fuels equivalents, they still present major challenges.

First, renewable generation is intermittent [7] [8], which means that it is challenging to accurately predict the amount of power those sources can produce over a given timeframe. For example, cloudy skies reduce solar power generation, and low wind speeds limit the performance of wind turbines. Conversly, more sunlight or stronger winds result in increased production, unless the systems are already running at maximum capacity. This intermittency creates engineering challenges in planning electricity generation [9].

Secondly, while coal, gas and nuclear power plant can have outputs in the hundreds, or even thousands of megawatts, renewable power plants can have much lower nominal power, sometimes just a few megawatts [8]. Additionaly, compared to their fossil fuel versions, renewable sources are more prone to be connected to the electrical grid at both transmission and distribution levels, which is why they are referred to as *Distributed Generation* (DG) [10] [11].

Moreover, renewable energy sources like photovoltaic (PV) systems directly produce DC power, while modern wind turbines generate variable frequency AC power that goes through a DC stage before being sent to the AC grid [12].

A bipolar DC network is a type of electrical power distribution system that uses

direct current [13]. It involves transmitting power through two DC poles, labelled positive and negative. This configuration provides two different voltage levels: the voltage of each pole and the voltage across both poles. One significant advantage of DC networks is their ability to integrate energy sources and storage without requiring conversion from a DC to an AC power. This flexibility is crucial as the use of energy sources and storage, such as solar panels, wind turbines, batteries and fuel cells, is expected to increase in the future.

The considered bipolar DC networks in this master's thesis are microgrids. The term *microgrid* refers to a localized and small-scale electrical network that can operate independently (in islanded operation) or in conjunction with a larger-scale electrical grid [14]. Hence, bipolar DC microgrids are expected to help increase the integration of renewable energy sources in local networks, removing the intermittent power stress from the main AC electrical network, all the while eliminating the requirement for additional DC-AC stages between DC power sources and the grid.

Motivation for this thesis

Although bipolar DC microgrids have advantages over AC networks or unipolar DC networks when it comes to flexibility and renewable energy sources integration, their development is facing significant technological challenges [13]. Voltage unbalance is one of them, affecting both the operation and overall performances [15]. Uneven load distribution can cause voltage deviations in the poles of the grid. Those deviations can lead to uneven power distribution, increased losses and damage the equipments or the microgrid itself. Therefore, it is crucial to develop solutions to keep DC microgrids in a balanced operational state.

Despite the importance of voltage unbalance mitigation, there is a lack of comprehensive studies on this matter. This thesis defines the voltage unbalance problem in a bipolar DC microgrid and digs into the literature to list and to classify the existing solutions to this problem. Then, this paper opens a discussion about how to choose between all existing topologies, depending on the use case. Finally, results from Matlab (Simulink) simulations give suggestions for the potential positions of those devices and how to integrate them in a bipolar DC microgrid.

This thesis takes the *MIRaCCLE Project* [16] as inspiration. This project of bipolar DC microgrid in Wallonia, in Belgium, aims to connect industries together through a local grid. The influence of this project on this work is mainly on the dimensioning of the simulation network regarding the lengths of the lines and the power profiles of the loads, as explained in section 5.

Research questions and objectives

The following research questions are intended to assist in achieving the objectives of the thesis:

1. What is a voltage unbalance in a bipolar DC grid?
2. What are the existing solutions to the voltage unbalance problem in a bipolar DC grid?
3. How to choose between the solutions to the voltage unbalance problem?
4. How and where to integrate them in the grid?

It is hoped that the suggested answers to those research questions will open perpectives and serve as basis for future researchs to be built on.

Thesis structure outline

This thesis is divided in several chapters and sections:

Chapter 1 serves as a literature review and aims to provide a comprehensive understanding of the voltage unbalance problem and its consequences. The chapter then proceeds to discuss the existing solutions available in the literature. To organize the diverse range of solutions, the chapter classifies them in two categories: Voltage Balancers (VB) and Current Redistributors (CR). A section is dedicated to explain the differences and similarities between the two, shedding light on their respective strenghts and limitations. Following this comparison, a method to derive voltage balancer topologies from common DC-DC converters is explained. Then, this chapter continues by conducting a thorough literature review on the comparison of the different voltage balancers and current redistributors solutions. It examines various studies and reasearch papers to assess the performance, effectiveness and applicability of these approaches. Finally, based on those findings, the chapter concludes by selecting specific topologies to be used in the simulations.

Chapter 2 focuses on the design and adaptation of the previously selected topologies to ensure their suitability for the simulations. It encompasses the necessary steps to make these topologies practical and functional, while also providing an explanation of the components sizing and choices involved in the design process.

Chapter 3 elucidates the methodology employed for the simulations, taking into account various aspects involved. It begins with describing the testbench used for the simulations. Then, a description of the simulations scenarios is given, in addition to

the different used criteria to evaluate the performance and stability of the simulated bipolar DC microgrid. Finally, a comprehensive list of the assumptions and limitations that might influence the results is given and described.

Chapter 4 presents and discusses the simulation results for the considered scenarios. This chapter is concluded with a summary of the current state of standardization for bipolar DC networks, providing a perspective on the matter.

Chapter 5 concludes this thesis by summaryzing the main results and what this work is believed to bring to the field of electrical engineering. Finally, future research topics and ideas are presented.

Chapter 1

Voltage Unbalance

This chapter focuses on the voltage unbalance problem in bipolar DC microgrids and explores various solutions proposed in the literature to mitigate this issue. It aims at providing both a state of the art and a basis on which it is possible to choose, design and simulate those solutions.

1.1 Voltage unbalance problem

As seen previously, one of the power quality issues associated with a DC microgrid is the voltage unbalance problem. The voltage balance is achieved when both the positive pole and negative pole voltages are equal to each other and to half of the system's total voltage. This is shown in Figure 1.1.

This problem arises when faulty control equipments operate on the grid, when the line impedances are not the same or when there is an unequal distribution of the power (consumed or produced) between the two poles [17]. While the two first causes of voltage unbalance shouldn't arise and are the consequences of faulty behavior, the last reason is something that is allowed, and most likely, to arise. The process of designing

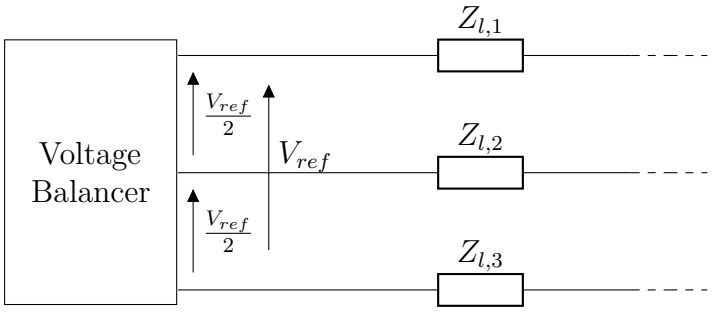

Figure 1.1: Voltage balance in a bipolar DC microgrid

a bipolar DC microgrid need to take into account this possibility.

The unequal powers flowing through the two poles can be caused by an unequal distribution of the loads, an unequal distribution of the distributed generation or a combination of both. An unequal distribution of the power between the cables will lead to two consequences.

The first one is linked to the voltage divider created by the loads and generation units between the positive and negative wires as seen in Figure 1.2. Depending on the power each of those components of the microgrid consume or produce, they will have an equivalent impedance as seen by the grid. If the powers exchanged between the two poles are unequal, then the equivalent impedance of the two poles will be different and the voltage drop associated with each of them will be unequal. In the case of a balanced bipolar DC microgrid, those voltage drops would need to be equal. Unequal distribution of the loads also leads to the magnitude of the currents flowing in the wires to be different. This causes different voltage drops amongst the transmission lines, resulting in unequal voltages for the poles of the downstream nodes.

Having different voltages amongst the two poles can lead to over- or undervoltage. This can have adverse effects on the connected equipments that can go from reduced lifespan to completely burning and destroying them. It can also trigger safety systems of some sensitive devices and disconnect them from the microgrid, which is not the expected behavior of the electrical network. From the microgrid operator point of view, the components of the grid can also suffer because of those voltage deviations.

Secondly, it is necessary to consider the currents flowing in the different wires. In the case of a balanced distribution of the powers amongst both poles, the current flowing in the positive cable will be the same as the current flowing through the negative cable in magnitude. Since their magnitude are the same, the current in the neutral wire has to be zero by Kirchhoff's current law. This leads to equal voltage drops amongst the transmission lines for the positive and negative wires, while the voltage drop accross the neutral transmission line's impedance will be zero, due to the zero current. In the case of an unbalanced scenario, the current flowing in the positive wire will be different than the current flowing in the negative wire. This will create a non-zero current flowing in the neutral wire to make up for the difference between those currents. The voltage drops for each transmission line will hence be different, making the voltage deviation bigger. The voltage drop over the transmission line is found with Ohm's law $\Delta U = R \times I$.

Figure 1.2 shows a simple representation of the current flowing through the transmission lines of the bipolar DC microgrid. At this point, we only consider steady state operation and the line's inductances are omitted. The losses on the lines can be

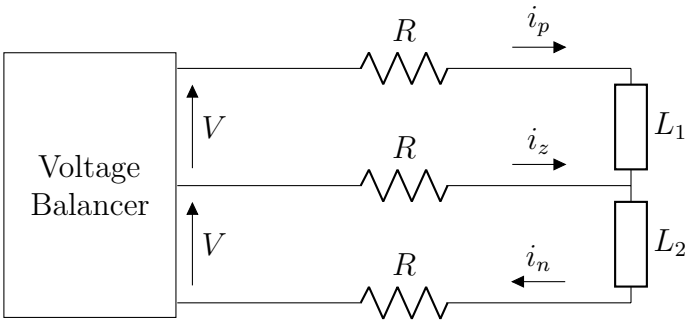

Figure 1.2: Simple steady state representation of a bipolar DC microgrid with the line resistance R and loads L1 and L2

expressed as in equation 1.2, since losses in a resistor are expressed as $P_{losses} = R \times I^2$. The impedance of the lines should be the same by design, equal to R in this example.

$$P_{\text{losses}} = i_p^2 R + i_n^2 R + \Delta i^2 R \tag{1.1}$$

$$= R\left(i_p^2 + i_n^2 + \Delta i^2\right) \tag{1.2}$$

where $\Delta i = i_n - i_p = i_z$ is the difference between the currents flowing in the positive and negative wires. Graphic representations of the losses are shown in Figure 1.3a and 1.3b where the z-axis values are given just in a representative manner to see the order of magnitude. It can be seen that for any current flowing through one of the wire, the losses will be minimized if the same current flows in the opposite wire.

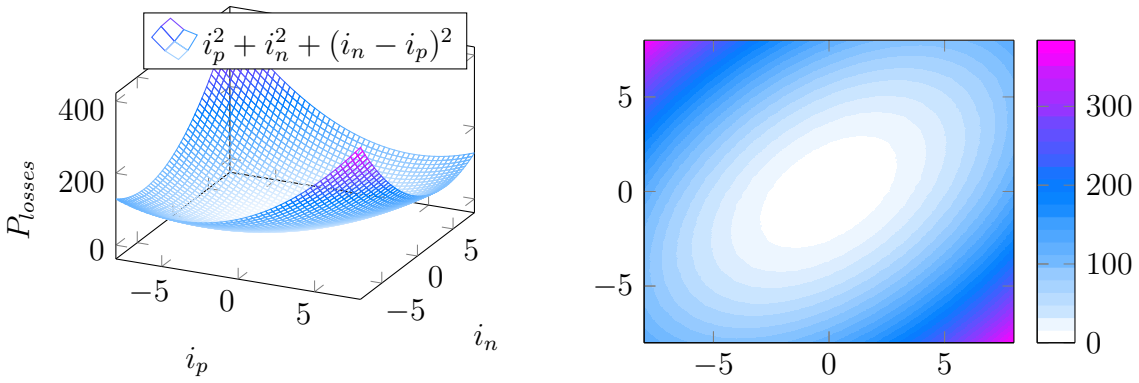

(a) 3D plot

(b) Contour plot

Figure 1.3: Losses curve depending on the distribution of the currents between the cables.

This result shows that the transmission losses will be at their minimum if the currents flowing in the positive and the negative wire are the same. In other words, the transmission losses will be minimized if the current in the neutral wire is zero, and thus

that the microgrid voltages are kept balanced.

1.2 Solutions to voltage unbalance

There are several solutions to prevent voltage unbalances. First, preventive solutions exist but are sometimes difficult implement. Connecting the loads and generation unit in a balanced way between the two poles (either directly between the positive and negative wire, or using the neutral wire as well) would prevent voltage unbalance. In practice, loads and distributed generation units don't have the same power and/or voltage ratings, making it difficult to distribute them equitably. In addition, the bipolar DC microgrid concept aims at being flexible for the end user [18]. This means that a very rigid code of how the loads should be connected to the network goes against this idea.

The most discussed solution lies in the use of extra power electronics devices in the microgrid [18]. Those additional devices can be split in two main categories. The first category includes modified DC-DC converters connected inside the grid between the three wires to redirect the excess power from one pole to the other [2]. Those devices are called voltage balancers, and sometimes current redistributors. The distinction between the two is explained later in section 1.3. The second category is also modified DC-DC converters but connected as the interface between the microgrid and the loads and power generation units. They are referred as loads and generation units with bipolar connection. Through this new interface, they will be connected to all three wires at the same time. The power electronics devices will dynamically draw or supply power from/to the grid by exchanging power with both poles at the same time, depending on the power balance.

Voltage balancers can be operated either in a centralised or a decentralized architecture. The first one, as illustrated in Figure 1.4b, is connected right after the main power supply of the bipolar DC microgrid. In this case it is represented as a three-phase network (that could be a generation unit or the main electrical grid) and a rectifier. In an islanded microgrid, it could be an energy storage system, like a battery for example. The voltage balancer receives as input an unipolar DC voltage. In this position in the grid, the role of the centralized voltage balancer is to create the neutral wire's voltage at half the voltage of the unipolar input. Furthermore, its dynamic operation should maintain the voltage balance between the two poles it creates while the power distribution is changing.

The decentralized architecture, also called standalone voltage balancer, operates in the same way but can be connected anywhere in the microgrid. It doesn't take any

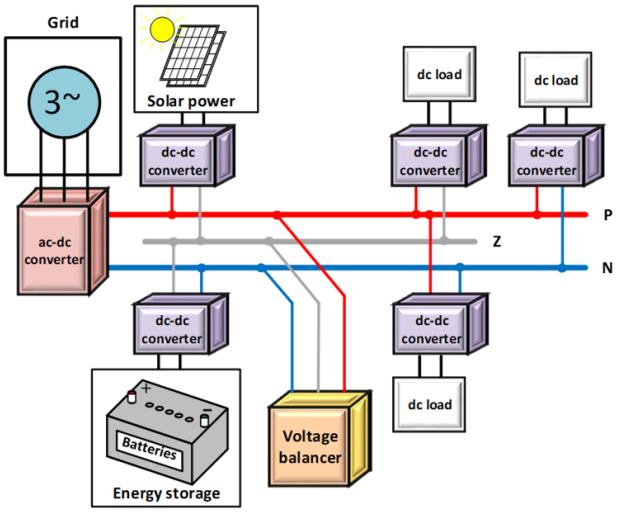

(a) Example of bipolar DC microgrid forming by using only a standalone voltage balancer

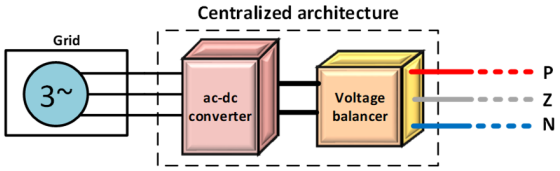

(b) Centralized architecture

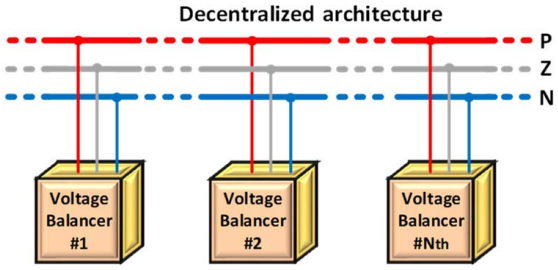

(c) Decentralized architecture

Figure 1.4: Voltage balancers and their placement in a bipolar dc microgrid [1].

input and just connects to the three wires. Unlike the centralized voltage balancer, there is no need to open the lines since this one has a parallel connection instead of a series one. It's main purpose is to keep the voltage balance in a remote location in the microgrid, not necessarily close to the main power supply.

It is also possible to create a bipolar DC microgrid by using only standalone voltage balancers. In this case, represented in Figure 1.4a. The advantage of this kind of architecture is that it would be possible to create a bipolar DC microgrid right from within a DC grid, where the loads could specifically need lower voltages. Since this thesis deals with DC microgrids that are only designed in a bipolar way, this solution won't be discussed in this work.

1.3 Voltage balancer vs current redistributor

In the literature, both voltage balancers and current redistributors are mentioned as solutions to the voltage unbalance issue. The actual difference between the two is

somewhat less explained. A voltage balancer is expected to keep the voltage of both poles balanced. On the other hand, a current redistributor redistributes the current flow in the microgrid to make it evenly shared between the positive and negative pole, constraining the neutral current to be zero.

In order to control a voltage balancer, the control system compares one pole's voltage with a reference voltage that is half of the total voltage accross the two poles. Whereas for a current redistributor, the control system aims at keeping the neutral current of a line to zero. The first one is voltage controlled, while the second one is current controlled. Furthermore, some architectures are specific to current redistributors, like explained in section 1.6. Thus, if we connect a voltage balancer somewhere in the microgrid where the currents are already unbalanced, there is no guarantee that the currents distribution between the cables will be symmetric. The same goes the other way around. A current redistributor connected at some node in the microgrid where the voltages are unbalanced will not necessarily restore this balance.

Nonetheless, there is a situation where both voltage balancers and current redistributors give the same result even though they are different in the way they regulate voltage and current at a certain node. Indeed, a current redistributor ensures equal current flows in the positive and negative wires, leading to equal voltage drops on the line from the upstream node to the point of connection of the balancing device. If the upstream node has its voltages balanced, then the connection node has the same property. This results would have been achieved by adding directly a voltage balancer at the same position. Using a voltage balancer in the same scenario equilibrates the currents in the line to maintain voltage balance. In other words, using a voltage balancer or a current redistributor downstream of a voltage balanced node has the same consequences on the currents and the voltages. Appart from this specific case, nothing guarantees that they behave in the same ways.

1.4 Topology deduction of voltage balancers

The main function of a voltage balancer is to ensure power balance between the positive and the negative pole of the bipolar configuration of the DC microgrid. Essentially, it allows power to flow from one pole to the other, depending on the load conditions. The operating principle can be compared to the one of a bidirectional DC-DC converter [2].

Figure 1.5a shows the general circuit of such a converter that has reverse input and output polarities. It has a positive input voltage, between the input ($+V$) and neutral wire (L_N), and also a negative voltage between the output ($-V$) and neutral wire (L_N). Figure 1.5b shows exactly the same circuit but rotated clockwise of 90° and

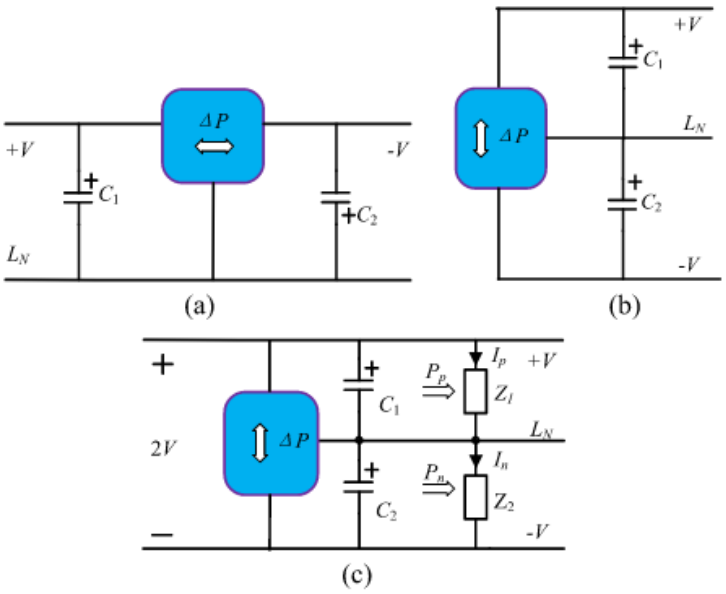

Figure 1.5: Topology deduction of voltage balancer from a bidirectional polarity reversal DC-DC converter [2]

flipped verticaly. From this circuit, adding an unipolar source on the left side connected between $+V$ and $-V$ completes the power supply of the circuit. The two poles of the bipolar DC network are located between $-V$ and L_N, and L_N and $+V$. This is shown in Figure 1.5c, which corresponds to the general circuit of a voltage balancer. The block containing the power exchange device (ΔP) is the DC-DC converter.

This DC-DC converter has to be bidirectional to allow power to flow from one pole to the other, thus able to respond to both unbalanced load conditions. Those conditions are the following: when the loads require more power on the positive pole, and when the loads require more power on the negative pole. It also needs to have reversed input and output polarities (see Figure 1.5), i.e. a dual-port polarity reversal converter.

With this knowledge, it is possible to deduce several topologies of potential voltage balancers based on bidirectional reversed polarities DC-DC converters. An example is given in Figure 1.6 with a bidirectional Buck/Boost-type DC-DC converter in Figure 1.6a, and the corresponding voltage balancer in Figure 1.6b.

Several DC-DC converters topologies can be considered as potential voltage balancers. To name but a few: Buck/Boost-type, Ćuk, Super-SEPIC and Super-Zeta. The next section performs a more in-depth analysis of the existing voltage balancer found in the literature.

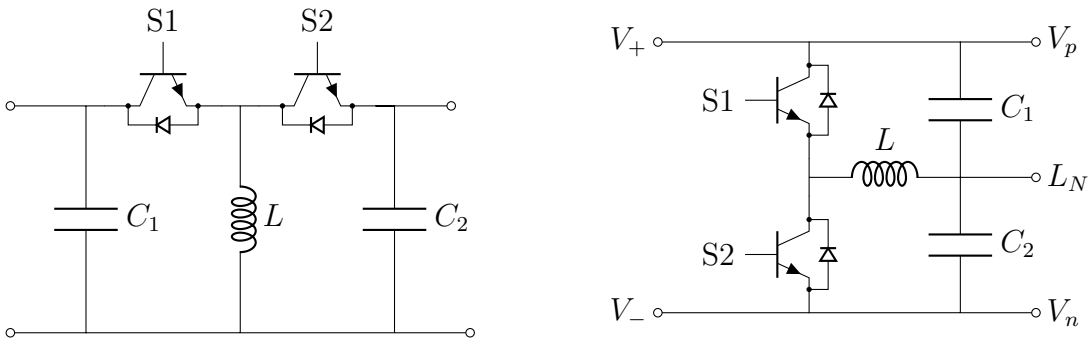

(a) Buck/Boost-type bidirectional DC-DC converter

(b) Buck/Boost-type (half-bridge) voltage balancer

Figure 1.6: Example of topology deduction of a voltage balancer based on a Buck/Boost-type DC-DC converter

1.5 Comparison of the voltage balancers in the literature

Several scientific papers analyse different topologies of voltage balancers. Since the interest about bipolar DC microgrid is rather new, the scientific research is still at its beginning and rather scarce. To the author's best knowledge, the literature can be split in two main types of documents. Some suggest new topologies and analyse their proper functioning on very small testbenches [2] [19] [20] [21] [22] [23] [24] [25], while other try to make comparison and to classify the voltage balancers that have been studied individually in the first category of papers [18] [1] [3]. This section first presents the potential solutions found in the literature, then compares them as well according to different criteria chosen for the context of voltage balancing. Using this section's work, it is then possible to choose the best topologies for the simulations done in the next chapters.

As stated in Section 1.4, most bidirectional DC-DC converters can be modified to obtain a voltage balancer. As for DC-DC converters, some design limitations and tradeoff need to be taken care of, such as:

- Shoot-through problem
- Current ripple (dynamic response)
- Number of components
- Control strategy
- Voltage regulation

Shoot-through problem The shoot-through problem refers to the short-circuit current that can flow from the positive to the negative pole of an half-bridge DC-DC converter and the similar topologies where cascaded switches are connected in series between the two poles. If the control of the switches is faulty and creates either wrong switching sequences, or delays the switching in some manners, it can lead to both switches being in closed positions. This event, even for a very short period of time, can cause a short circuit that could permanently damage the balancing device and other grid equipments.

An important note is that the shoot-through problem is actually not really relevant. It is possible to implement a gate driving circuit that prevents this issue. It is not digital, and only based on two resistances and a diode, as shown in Figure 1.7. It allows the current driving the switching device to charge slower and discharge faster due to different equivalent resistances opposing the current flowing to and from this device. This will create a short dead-time during which both switches will be in an open position. In the following subsection, the shoot-through problem will still be considered a potential issue while comparing balancing topologies to stay as complete as possible, even though in practice it can be easily mitigated.

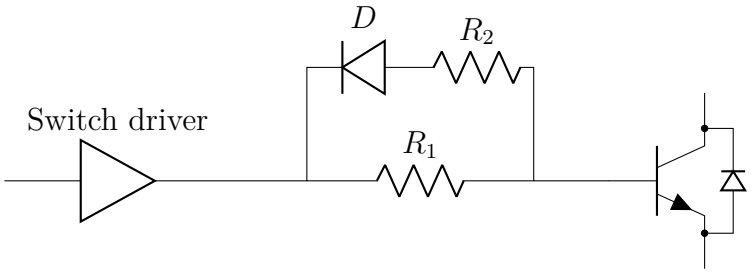

Figure 1.7: Delay inducing switching device gate driving circuit in order to prevent the shoot-through problem

Current ripple The current ripple refers to the current flowing in the wires due to the inductance storing and releasing energy from the action of the switching devices. The bigger this ripple, the bigger the capacitances needed as output filter in order to keep relatively more stable voltages and currents in the lines. By adding bulkier capacitances, the dynamic response is slower.

Number of components The number of components used for each topology influences their cost and the complexity of the design. It also decreases the mean time before failure.

Control strategy Some topologies with less switches and symmetric architectures can have more straighforward control strategies than other complex topologies. In this thesis though, the emphasis is placed on the voltage balancing devices, where to place them and assess their global performance in mitigating voltage unbalance. Their control system in this paper are thus rather simple.

Voltage regulation While voltage balancers keep voltage balance accross the three bipolar DC microgrid's wires, sometimes the total voltage between the positive and negative pole can be lower than the nominal one. Voltage regulation refers to the ability to keep this voltage at nominal value. It is usually done by combining a voltage balancing device with a regulating device, since most standard voltage balancing topologies cannot further regulate the voltage levels, mostly because they don't aim to by design.

The voltage balancers found in the literature can be classified in differrent categories: nonisolated voltage balancers, isolated voltage balancers and standalone voltage balancers. Additionaly, two other solutions related to voltage balancing exist: AC to DC balancing interfaces and loads, sources and ESS with balancing capabilities.

1.5.1 Nonisolated voltage balancers

Nonisolated voltage balancers refer to voltage balancers that don't have a galvanic isolation between the power supply and the rest of the microgrid. Section 1.5.2 explains why some bipolar DC microgrids architectures might need a galvanic isolation. The kind of voltage balancers discussed here is connected in series with the main unipolar power supply and the bipolar DC grid. It creates the neutral wire's voltage at the middle of the total voltage and dynamically keeps it balanced.

Figure 1.8 [1] shows a summary of the main DC-DC converters that have been modified to be used as voltage balancers. Figure 1.8a shows a simple Buck/Boost-type, also called half-bridge voltage balancer. As it is the combination of a Buck and Boost converter, it can either boost or buck the voltage accross the poles to balance the bipolar DC voltages. Figure 1.8b shows the circuit of an improved version of the Buck/Boost-type voltage balancer that is able to regulate the unipolar DC voltage provided as input in addition to maintain the voltage balance. Those two topologies suffer from the shoot-through problem and several derived topologies exist.

Figure 1.8c is one of those other topologies. it is called the dual Buck/Boost voltage balancer. It doesn't suffer from the shoot-through problem because even though both switches would be closed at the same time, there would not be a direct path from one pole to the other. On the other hand, it required more components than the simple

half-bridge voltage balancer.

Following the same idea, Figure 1.8d, Figure 1.8e and Figure 1.8f are respectively derived from the Ćuk, Super-SEPIC and Super-Zeta DC-DC converters. All three of them eliminate the shoot-through problem at the expense of a greater number of components.

The previous circuits constitute a set of basic voltage balancer topologies that can be improved depending on the use case. Figure 1.8g for example is an interleaved half-bridge voltage balancer. Thanks to the interleaved architecture, the average current flowing from the inductors to the capacitances can be zero. The size of its capacitances C_1 and C_2 can thus be reduced, offering a better dynamic response. Similar topologies with n legs have been developed as well. Figure 1.8h, Figure 1.8i and Figure 1.8j show voltage balancing topologies for high voltages. By putting switches in series, "three-level converters" (3L) are obtained and each switch withstands only half of the total voltage. Figure 1.8i shows the three-level half-bridge voltage balancer connected to a Neutral-Point Clamped (NPC) AC-DC converter. The purpose is to show that a connection with an AC network is possible as long as there is a conversion from AC to DC, here implemented with the NPC.

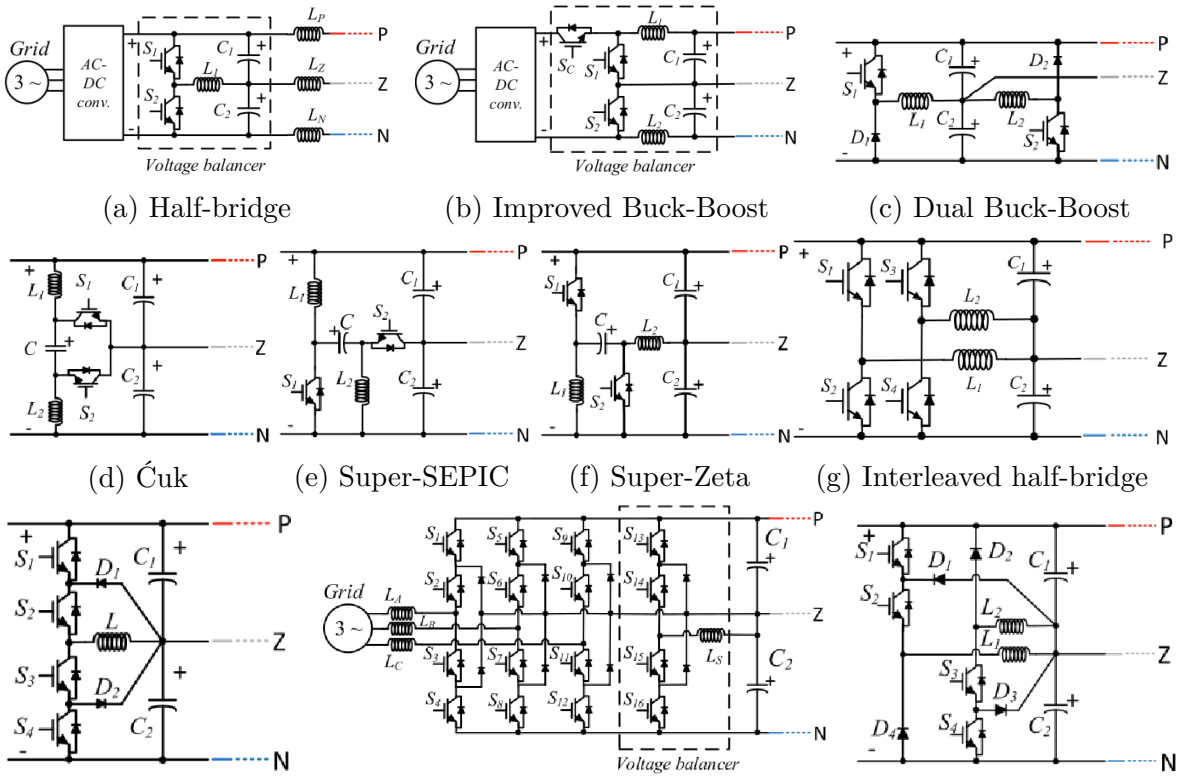

(a) Half-bridge (b) Improved Buck-Boost (c) Dual Buck-Boost

(d) Ćuk (e) Super-SEPIC (f) Super-Zeta (g) Interleaved half-bridge

(h) 3L half-bridge (i) 3L neutral-point clamped (NPC) and 3L half-bridge (j) 3L dual Buck-Boost

Figure 1.8: Summary of nonisolated source connected voltage balancers [1]

1.5.2 Isolated voltage balancers

For safety measures, some systems need galvanic isolation [26]. In order to obtain this isolation, it is possible to use a transformer between the two systems that need to be isolated from one another. It can also block currents induced by AC systems. Figure 1.9 shows an example of an isolated voltage balancer's topology connected to an AC system that would be the bipolar DC microgrid main power supply in this case. More details about those solutions are developped in Appendix A.

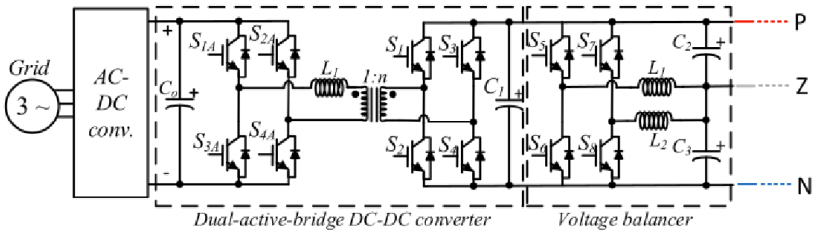

Figure 1.9: Example of isolated source connected voltage balancer [1]

1.5.3 Standalone voltage balancers

All nonisolated supply connected voltage balancers can be used as standalone voltage balancers. Indeed, voltage balancers are connected to the positive and negative poles, and create the neutral wire's voltage. It doesn't necessarily need to be connected to a power supply. Figure 1.10 illustrates the idea behind the concept of standalone voltage balancers.

The main use case of standalone voltage balancer is to maintain the voltage balance at specific nodes in the bipolar DC microgrid. Even though there is one voltage balancing device creating this bipolar architecture at the connection point of the main power supply (would it be an ESS or another AC, or DC, system), voltage unbalances might arise elsewhere due to unbalanced operation.

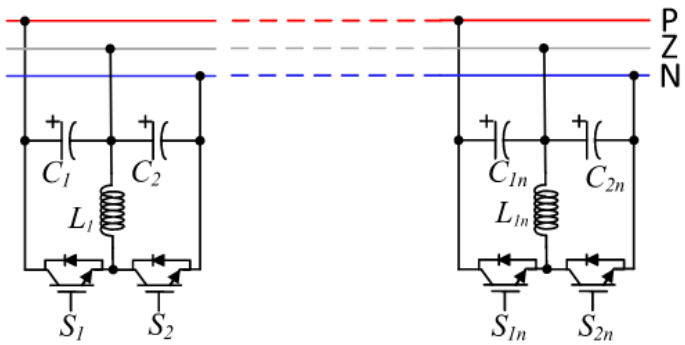

Figure 1.10: Standalone half-bridge voltage balancer [1]

The main difference between the voltage balancers discussed here and the ones described in subsection 1.5.1 is that the standalone voltage balancers don't aim to provide power to the node. Indeed, previously discussed topologies were connected to a power supply. They were also creating the bipolar architecture by creating the neutral line's voltage in addition to dynamically keeping it balanced. In the case of a standalone voltage balancer, the main goal is to maintain voltage balance.

Nonetheless, even though it is not in the research topics of this thesis, it would be possible to create a middle point with such voltage balancers in order to create a local bipolar grid within an unipolar DC grid, as depicted previously in Figure 1.4a.

1.5.4 Loads, sources and ESS with balancing capabilities

Here, a distinction between loads, sources and ESS should be done. Indeed, loads only draw power from the grid, sources supply power to the grid, and ESS should be able to both retrieve power from and supply power to the grid. The different architectures presented here will have some variations depending on the direction of the energy flow. The DC-DC converters that can serve as interface between the bipolar DC network and the sources, loads and ESS are developped in [1].

Sources Instead of using DC-DC converters to connect loads and sources to the grid, it is possible to consider using multiport DC-DC bipolar converter. Those topologies can be studied and controled to inject power in the pole with the lowest voltage [1] in order to mitigate the existing voltage unbalance at the node where it is connected.

To demonstrate the general idea behind such interface between the bipolar grid and the components connected to it, Figure 1.11 illustrates the different cases. When operating in an unbalanced way, the power should be injected in the pole with the lowest voltage. Figure 1.11a shows this case with the voltage of the positive pole being lower than the negative one, and Figure 1.11b shows the converse, when the negative pole's voltage is the lowest. In a balanced operation of the grid, the power should be injected equitably in both poles, as shown in Figure 1.11c. It is possible that the power from the source is bigger than the unbalanced power of the grid. If this power would be totally injected in the pole with the lowest voltage, then an unbalance would arise in the opposite pole. To prevent this, it is possible to inject power in both poles but in an unbalanced way, as pictured in Figure 1.11d and Figure 1.11e.

Loads The exact same principle as for power sources apply to loads. Figure 1.11 and the aforementioned explanation still holds, with that the power flow is reversed.

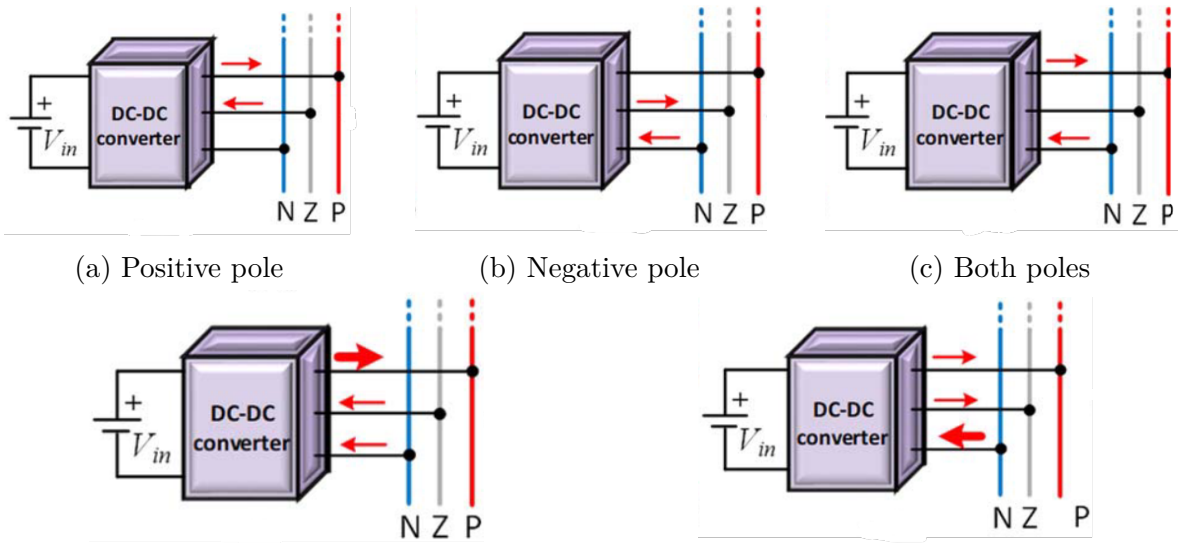

(a) Positive pole (b) Negative pole (c) Both poles

(d) Unbalanced injection (case a) (e) Unbalanced injection (case b)

Figure 1.11: Different operating principles of a bipolar DC-DC converter for sources connected to a bipolar DC microgrid [1]

Energy Storage Systems Figure 1.12 is showing the same power flows depending on the unbalance condition of the grid. This time, each situation is depicted in double, with the power absorbtion or supply. The unbalance condition in which each power transfer scenario happens is given in the captions. It is also possible to charge and discharge the ESS on both poles at the same time, with an uneven distribution of the power. This is shown in Figure 1.12d and Figure 1.12e.

1.5.5 AC to bipolar DC interface

Some topologies that don't come from DC-DC converters exist and are specifically designed to be used as an interface between three-phase AC systems and bipolar DC systems. They allow bidirectional power flows so that the two subsystems can both supply power to or receive power from the other one, depending on the operating conditions. Two of those topologies are the Two-level Voltage Source Controller (VSC) [18] (Figure 1.13a) and three-level Neutral-Point Clamped (NPC) [25] (Figure 1.13b).

Although those topologies have the advantage of doing the conversion from AC to DC and the voltage balancing in one step, they also suffer from a drawback. Indeed, as seen in Table 1.1, they need more components, especially the two-level Voltage Source Controller that requires a triple winding transformer.

After reviewing all the potential architectures for voltage balancers, Table 1.1 summarizes their most important characteristics. The "Shoot-through" column indicates if a voltage balancer topology can suffer from the shoot-through problem. The "Dynamic

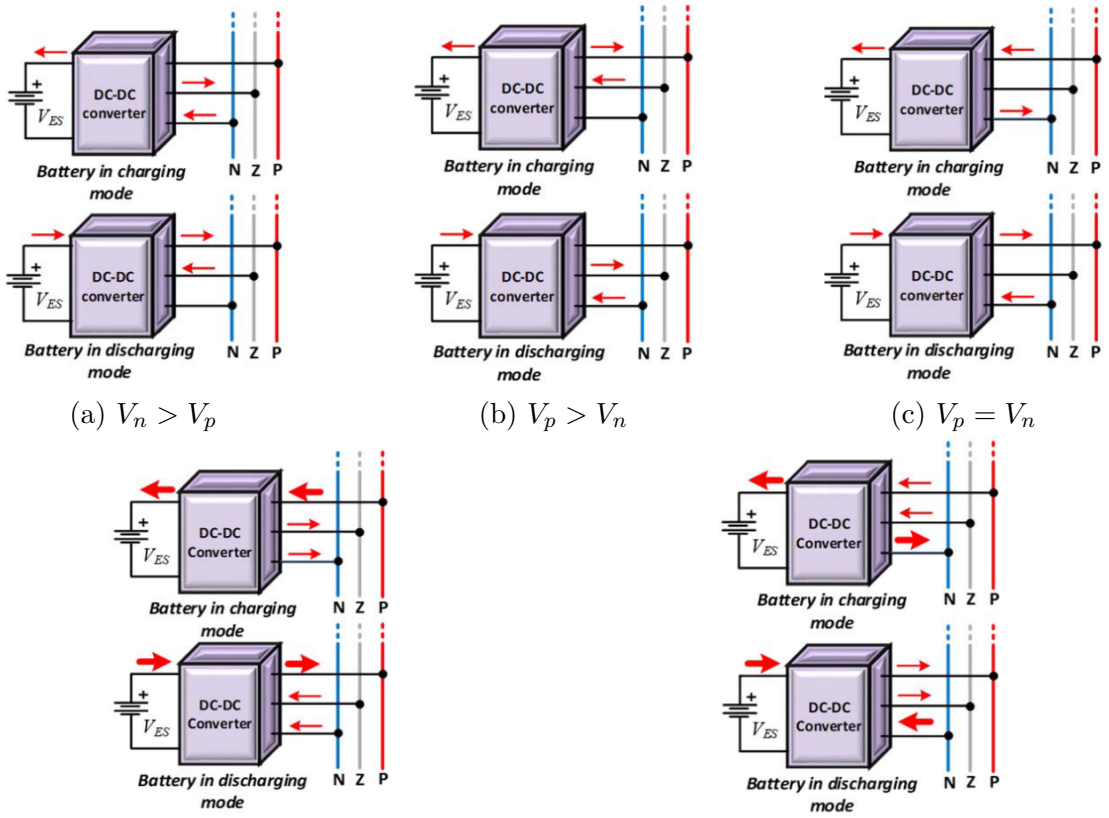

(a) $V_n > V_p$ (b) $V_p > V_n$ (c) $V_p = V_n$

(d) Mainly with the positive pole (e) Mainly with the negative pole

Figure 1.12: Different operating principles of a bipolar DC-DC converter for ESS connected to a bipolar DC microgrid [1]

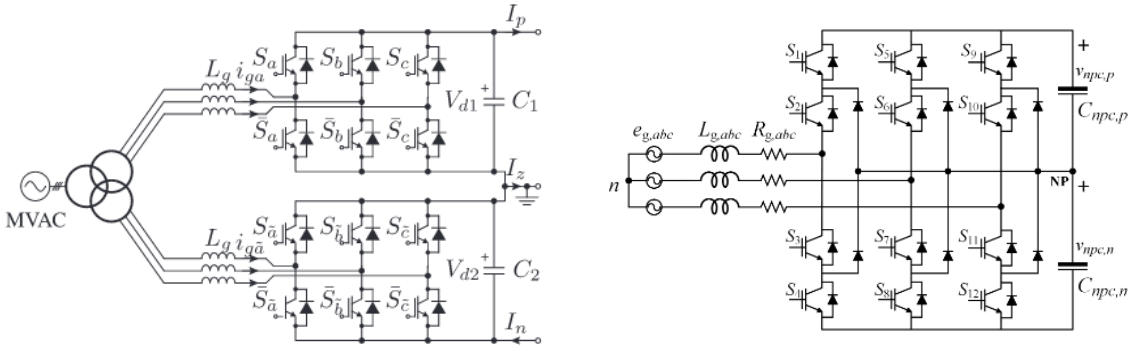

(a) Two-level Voltage Source Controller (VSC) [18]

(b) Three-level Neutral-Point Clamped (NPC) [25]

Figure 1.13: Main topologies creating a bipolar DC output from an three-phase AC system

response" is linked to the speed of the dynamic response, influenced by the size of the output capacitances, themselves depending on the amplitude of the ripple current. A "−" designates a relatively slow response compared to the other topologies, whereas "++" corresponds to a relatively faster response time. The number of components doesn't take their size into account. For example, the interleaved half-bridge voltage balancer has two capacitances, but of smaller sizes compared to the other topologies since the amplitude of the ripple current can be kept relatively small.

Voltage balancer	Shoot-through	Dynamic response	Voltage regulation	# of components		
				# Switches	# Self	# Caps
Half-bridge	Yes	+	No	2	1	2
Three-level Buck/Boost	Yes	+	No	4	1	2
Dual Buck/Boost	No	−	No	4	2	2
Ćuk	No	+	No	2	2	3
Super-SEPIC	No	+	No	2	2	3
Super-Zeta	No	+	No	2	2	3
Interleaved half-bridge	Yes	++	No	4	2	2
Two-level VSC	Yes	−	Yes	12	6	2
Three-level NPC	Yes	+	Yes	12	0	2

Table 1.1: Comparative table of some promising voltage balancer topologies that can be used to generate a bipolar DC network

1.6 Comparison of the current redistributors in the literature

In general, the literature on current redistributors is more limited than for voltage balancers. From [18], [3] and [27], it is possible to extract two main architectures for current balancing devices, shown in Figure 1.14.

The main idea behind those two topologies, and for current redistributors in general, is to control the middle wire's current. In practice, this is done by controlling the current flowing through the inductance like in the CR of type 1, or the multiple inductances

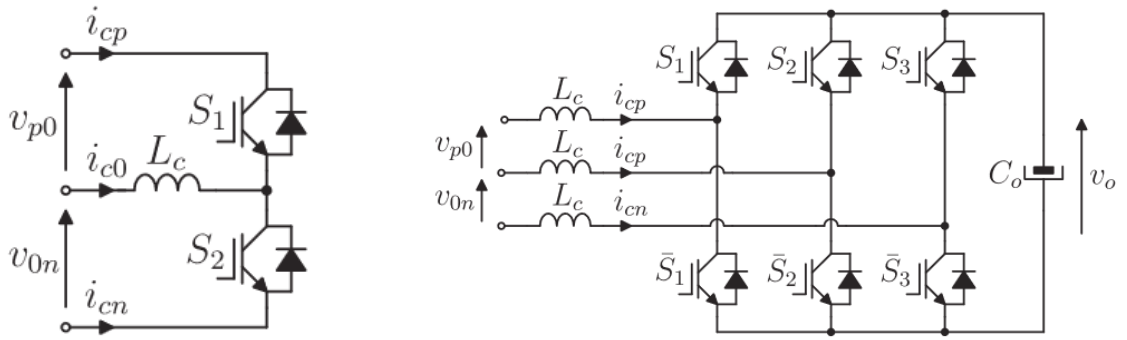

(a) CR type 1 (b) CR type 2

Figure 1.14: Two main topologies of current redistributors in the literature [3]

like in the CR of type 2. The main differences between the two, in addition to the number of components are the following: CR of type 2 is able to include energy storage at its DC link (C_o) and to operate with the loss of one DC line. This is gained at the cost of a more complex control system.

1.7 Choosing the right topologies

As seen in the previous sections, a lot of different topologies exist, with their own advantages and drawbacks. This section's goal is to choose which topologies are going to be used for the simulations in the next chapters. There is a need for topologies for a supply connected voltage balancer, a standalone voltage balancer, and a current redistributor.

1.7.1 Supply connected voltage balancer

The supply connected voltage balancer is the root of the bipolar DC microgrid. It creates the neutral wire's voltage and thus the network in itself. For this function, the half-bridge voltage balancer seems to be a good choice in this thesis. The small number of components compared to the other topologies and its large use in industry [20] makes it a good fit. Having less components ensures a lower risk of failure of the system and keeps it simple to work with. Additionaly, the author believes that using as little materials as possible is important in the context of global warming. Furthermore, the supply chain being under pressure at the time this thesis is written, using less components is believed to relieve this chain and reduce delivery time, ensuring quick realization of the projects including those devices.

Another topology, the interleaved half-bridge voltage balancer, seems interesting enough to be studied in this thesis. Even though it includes more components (see

Table 1.1) than the half-bridge topology, it limits the output current ripple. This allows to decrease the size of the circuit's capacitors.

1.7.2 Standalone voltage balancer

Since the circuits used for the supply connected voltage balancers can also be used as standalone voltage balancer topologies, the choice is the same than in subsection 1.7.1.

1.7.3 Current redistributor

Regarding the current redistributor topologies, the choice is made on the CR of type 1 for the same reason as mentioned in subsection 1.7.1. As it is explained later in chapter 3, no storage system that needs to be connected to a balancing device is used in the simulations. Furthermore, no fault analysis is conducted and thus the ability of the current redistributor of type 2 to operate under faulty behavior is not necessary in the scope of this thesis.

A summary of the chosen topologies is displayed in Figure 1.15.

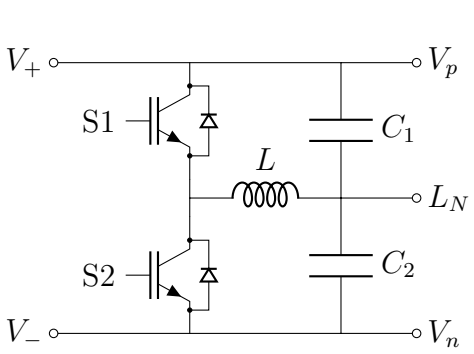

(a) Half-bridge voltage balancer

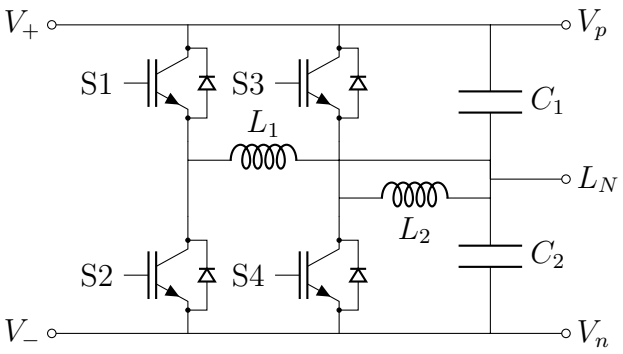

(b) Interleaved half-bridge voltage balancer

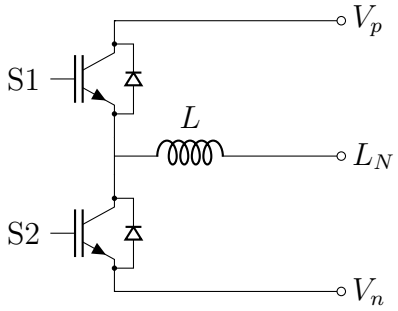

(c) CR type 1

Figure 1.15: Considered voltage balancer and current redistributor topologies for the simulations

Chapter 2

Design of the solutions

This chapter's goal is to design the different solutions, namely the different voltage balancers and the current redistributor, in order to use them in the final testbench. In the following sections, some design choices are made for the microgrid. The general parameters are the switching frequency of the switches (f_{sw}), the bandwidths of the voltage and current loops of the control systems (f_{BOI} and f_{BOV}), the nominal voltage of the poles and the power profiles of the connected loads.

The switching frequency is 10 kHz. As it will be seen later in subsection 2.1.2, this parameter will influence the maximum bandwitdh of the control systems and the sizing of the components, particularly the inductances. The bandwidths of the current loop of the controller needs to be at most equal to f_{sw}/π. This is necessary to keep the system stable and comes from the stability criterion of a PWM gate driver [28] [29] [30]. The voltage loop of the controller has a bandwidth of $f_{BOI}/10$ in order to keep both control loops independant and avoid interference between them [30]. Finally, the nominal voltage of the poles is chosen to be 750V, meaning that the total voltage of the network is of 1500V. This voltage has been chosen because it is the limit under which a DC system can be classified as a LVDC grid [31]. Those parameters are summarized in Table 2.1.

Symbol	Value	Unit	Description
f_{sw}	10	kHz	Switching frequency
f_{BOI}	$\frac{f_{sw}}{\pi} \simeq 3$	kHz	Current loop's bandwidth of the controller
f_{BOV}	$\frac{f_{BOI}}{10} = 0.3$	kHz	Voltage loop's bandwidth of the controller
V_p, V_n	750	V	Voltage of the poles

Table 2.1: Global parameters used for the simulations

The following subsections describe the design of an half-bridge voltage balancer, its interleaved version and its standalone version. Also, the half-bridge current redistributor is discussed. Finally, section 2.5 explains how to design a precharge circuit, necessary to connect those devices to the network during its operation. For each part, both the design of the circuit and the validation on a small testbench are discussed.

2.1 Half-bridge voltage balancer

The voltage balancer considered here is the half-bridge voltage balancer, shown in Figure 2.1. As explained in section 1.3, the main idea is to control the switches to load the inductance with one pole and reinject the excess power to the other pole. The control system driving the switches guarantees that the voltage balance is maintained dynamically during the network's operation.

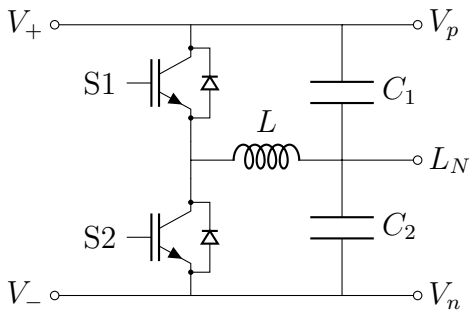

Figure 2.1: Half-bridge voltage balancer

2.1.1 Control system

In order to control the voltage balancer, both a current and a voltage loops are used, as displayed in Figure 2.2. The sensor gains K and K' are both unitary in the simulations used in this paper.

Once the values of the inductance L and the capacitor C are obtained, it is necessary to tune the different coefficients of the two PID blocks. This is done using the PID tuner tool provided by Matlab / Simulink, where it is possible to specify the desired bandwidth of the loop being tuned.

2.1.2 Components

Switching device

The choice of the technology used for the switching devices depends on the characteristics of the network they will operate within. According to [32], the main criteria to choose

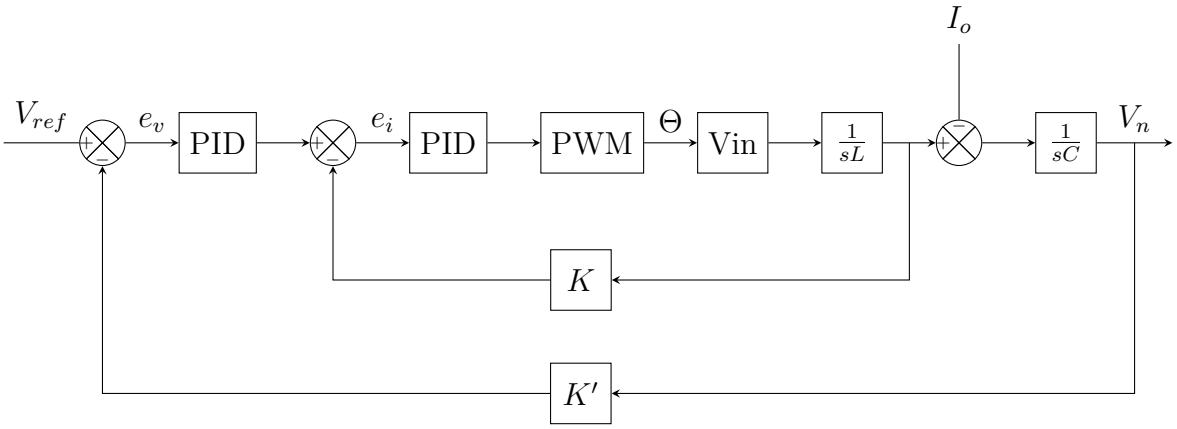

Figure 2.2: Block diagram of the control system of the voltage balancer.

between MOSFETs or IGBTs lies in the switching frequency and the voltage accross those switches. In this case, the switching frequency is 10 kHz and the voltage that they should withstand is about 750V. Hence, IGBTs seem to be the best suited solution.

Capacitance

When loads change their power profile during operation, the current they draw from the grid's power supply change. If this change is faster than the voltage balancer's control system, it is the capacitance of this device that is going to influence how big the voltage deviation is.

In order to size the capacitance, it is decided that the instantaneous current variation ΔI_o is limited to 25% of the total unbalanced power $I_{o,max}$. Following this maximum current variation, the voltage deviation ΔV_o needs to be limited to at most 1% of the pole's voltage, referred as V_o in this section. In a mathematical form, those criteria are:

$$\Delta I_o = 25\%\, I_{o,\max} \tag{2.1}$$

$$\Delta V_o = 1\%\, V_o \tag{2.2}$$

From those criteria, it is possible to deduce the corresponding criterion on the output impedance of the voltage balancer, which is given by Equation 2.3. A lower value of impedance would result in a lower voltage drop ΔV_o. The value obtained for Z_o is thus a maximum limit to respect the criterion.

$$Z_o \leq \frac{0.01\, V_o^2}{0.25\, P_o} = 0.04 \frac{V_o^2}{P_o} \tag{2.3}$$

In Equation 2.3 P_o is the unbalanced power supplied by one branch of the voltage balancer to the other. Based on the data available in section 5, and if we consider the power unbalance to be around 50% of the total power drained from the main power supply, then $P_o = 100$ kW. As it can be deduced from Equation 2.3, this can constitute a worst case scenario, since any lower unbalance power P_o will result in a higher minimum output impedance Z_o.

It is now possible to determine the maximum value of the voltage balancer's output impedance, which is given by Equation 2.4.

$$Z_o \leq 0.04 \frac{V_o^2}{P_o} = 0.04 \frac{750^2}{100 \times 10^3} = 0.225\,\Omega \tag{2.4}$$

The voltage loop of the control system presented in Figure 2.2 has a bandwidth of $f_{BOV} = 300$ Hz. Below this frequency, the controller will regulate the output voltage. Outside of this bandwidth, the control system is not fast enough to regulate the voltage. At higher frequencies, the output capacitance can play this role passively. The output impedance criterion can thus be expressed as

$$Z_o \leq \frac{1}{2\pi\, f_{BOV}\, C} \tag{2.5}$$

and the value of the capacitance

$$C \geq \frac{1}{2\pi\, f_{BOV}\, Z_o} \tag{2.6}$$

At this point, all values of Equation 2.6 are known. The minimum value of the voltage balancer's capacitance is therefore equal to 2.357 mF, as developped in Equation 2.7.

$$C \geq \frac{1}{2\pi \times 300 \times 0.225} = 2.357 \times 10^{-3}\ \text{F} \tag{2.7}$$

Inductance

The value of the inductance determines the amplitude of the current ripple flowing through this inductance. Indeed, Equation 2.8 depicts the voltage accross the inductance with regard to its current. Based on this relationship, Equation 2.9 expresses the amplitude of the current ripple Δi_L as a function of the voltage applied between the terminal of the inductance.

$$L\frac{di_L(t)}{dt} = V_L(t) \tag{2.8}$$

$$\Delta i_L = \frac{1}{L}\int_{\Delta t} V_L(t)\,dt \tag{2.9}$$

In a balanced scenario, which is the result of the expected behavior of the balancing circuit, each pole has a voltage of $V_{in}/2$. For the sake of simplicity of notations, the negative pole's voltage V_n refers to this value. Over one switching period going from 0 to T_{sw}, the voltage accross the inductance can be expressed as in Equation 2.10.

$$V_L(t) = \begin{cases} V_n, & \text{for } \Theta\, T_{sw} \\ -V_n, & \text{for } (1-\Theta)\, T_{sw} \end{cases} \tag{2.10}$$

The evolution of the voltage and the current of the inductance L are graphically represented on the graph of Figure 2.3 for a duty cycle Θ of 0.5.

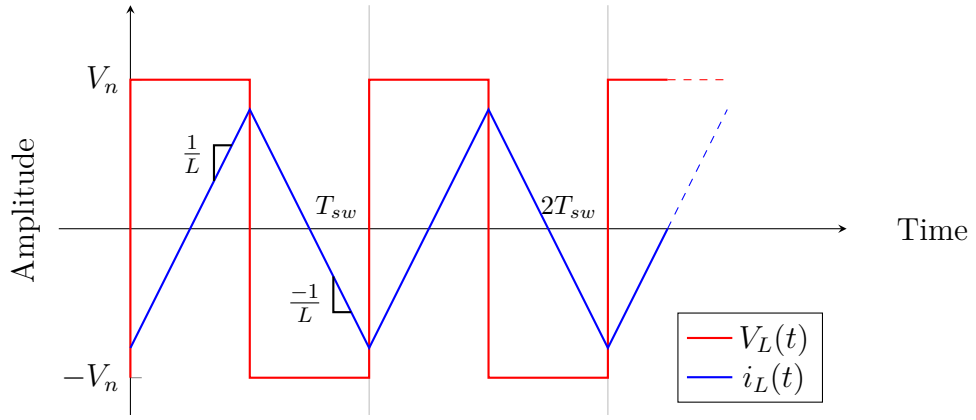

Figure 2.3: Voltage accross and current flowing through the inductance

In order to size the inductance L, it is possible to decide on a maximum current ripple knowing the voltage of the poles. Considering an unbalance power of 100kW as chosen previously to size the output capacitor, the current flowing through the inductance is $i_{L,ss} = 133.33$ A. The selected criterion is chosen to limit the amplitude of the ripple to 10% of the steady-state current's value. From Equation 2.9, we obtain the following expression:

$$L = \frac{1}{\Delta i_L}\int_{\Delta t} V_L(t)\,dt \tag{2.11}$$

$$= \frac{1}{0.1\, i_{L,ss}}\int_0^{\Theta T_{sw}} V_n\,dt \tag{2.12}$$

and the final minimum value of the inductance is found using $V_n = 750$ V, $i_{L,ss} = 133.33$ A, $\Theta = 0.5$ and $T_{sw} = 10^{-4}$:

$$L = \frac{750 \times 0.5 \times 10^{-4}}{0.1 \times 133.33} = 2.81 \times 10^{-3} \text{ H} \tag{2.13}$$

The values of the parameters of the design of the voltage balancer circuit are summarized in Table 2.2.

Parameter	Value	Unit
f_{sw}	10	kHz
L	2.81	mH
C	2.357	mF

Table 2.2: Sumary of the voltage balancer's paramaters

2.1.3 Behavior without balancing

Before assessing the performance of the voltage balancer discussed above, it is interesting to observe the behavior of the bipolar DC network if no balancing device is used. The easiest passive way of building a bipolar DC network from a single unipolar DC source is to place two capacitors in series between the negative and positive wires, creating the neutral wire's voltage in the middle.

This solution is displayed in Figure 2.4. This circuit is the reprentation of a simple network. The two capacitors are located between the unipolar main power supply and the bipolar network. The bipolar network consists of a transmission line and loads. The transmission line is a RL impedance. Even though the network is DC, an inductance in the line is needed to take into account the different behavior of the microgrid when voltages and currents are varying. The loads are of two types: constant baseload of 100kW on each pole, and three varying loads.

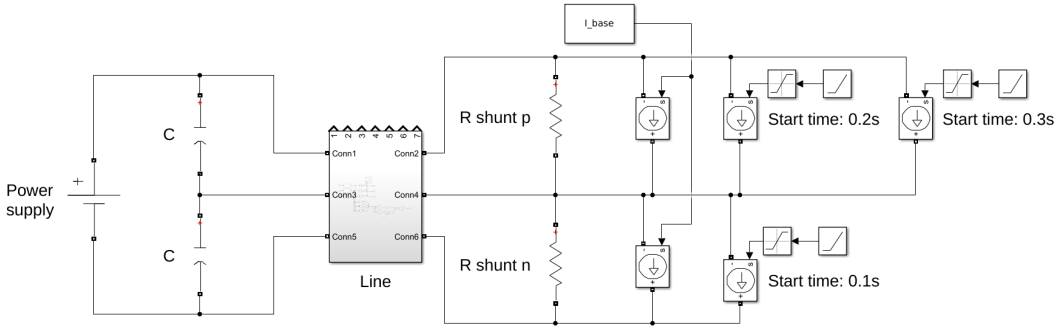

Figure 2.4: Naive implementation of a bipolar DC network using capacitors

The loads are represented as simple constant current loads. In order for the simulation software to be able to run the simulation, shunt resistors have been added on each pole, with a value of $10^5\,\Omega$. Indeed, putting an inductance in series with a current source was causing wrong behavior of the software. The varying loads have different starting times, going from 0 ampere to their nominal current with a slope of 5×10^4, in order to simulate a rapid turn on.

The first load to turn on is connected to the negative pole at 0.1 second, L_1. Then, two loads on the positive pole turn on, L_2 and L_3. First at 0.2 second and then at 0.3 second. This is shown in Figure 2.5. The powers drawn by the loads are given in Table 2.3.

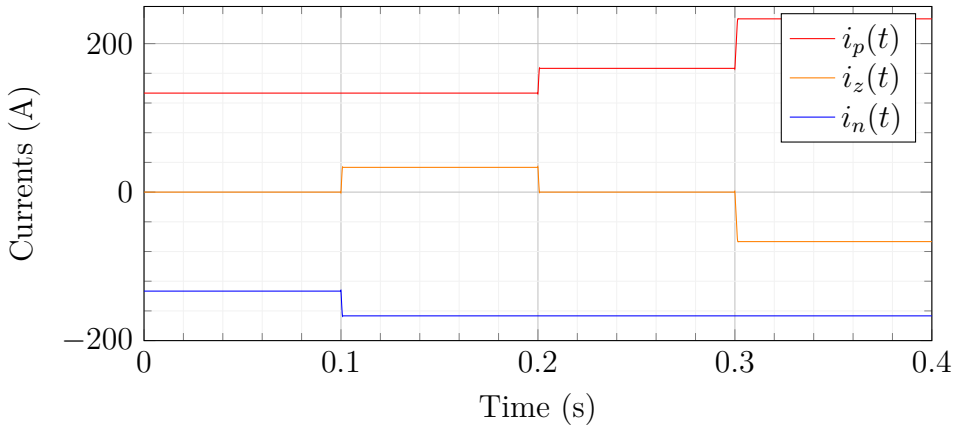

Figure 2.5: Line currents of the simple DC bipolar network

Load #	Voltage [V]	Current [A]	Power [kW]	Starting time [s]
Baseload	750	133.33	100	0
1	750	33.33	25	0.1
2	750	33.33	25	0.2
3	750	66.67	50	0.3

Table 2.3: Loads power

In order to predict the behavior of such a system, it is necessary to understand how the capacitors are going to influence the voltages. The voltage and current relationship for a capacitor is ruled by Equation 2.15.

$$i_C(t) = C\frac{dv_C(t)}{dt} \tag{2.14}$$

$$\Leftrightarrow v_C(t) = \frac{1}{C}\int i_C(t)dt \tag{2.15}$$

As long as the loads on both poles are drawing the same power, the currents in the positive and negative wires are equal. This means that no current is flowing through the neutral wire and the capacitors have no influence on the circuit at steady state. On the other hand, if an unbalance occurs, then the neutral wire's current will charge or discharge the capacitors. Calling this current $i_C(t)$ and using Equation 2.15, the capacitors bahavior can be deduced. Since the loads are constant current loads, the integral of the current acting on the capacitors determine their voltages. This behavior is displayed in the graph of Figure 2.6.

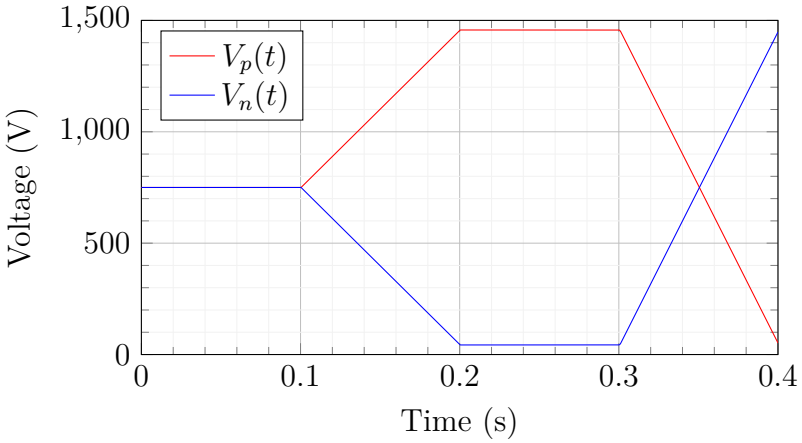

Figure 2.6: Voltage levels without any balancing device

2.1.4 Validation

The circuit used to validate the design is the reprentation of a simple network, containing the power supply, the voltage balancer, one distribution line and the loads. This network is displayed in Figure 2.7.

Regarding the voltages, Figure 2.8a shows the evolution of the voltages of the poles while the loads are turning on. As expected, the voltages change when an unbalance arises. The voltage of the pole that experiences a rise in power demand drops due to

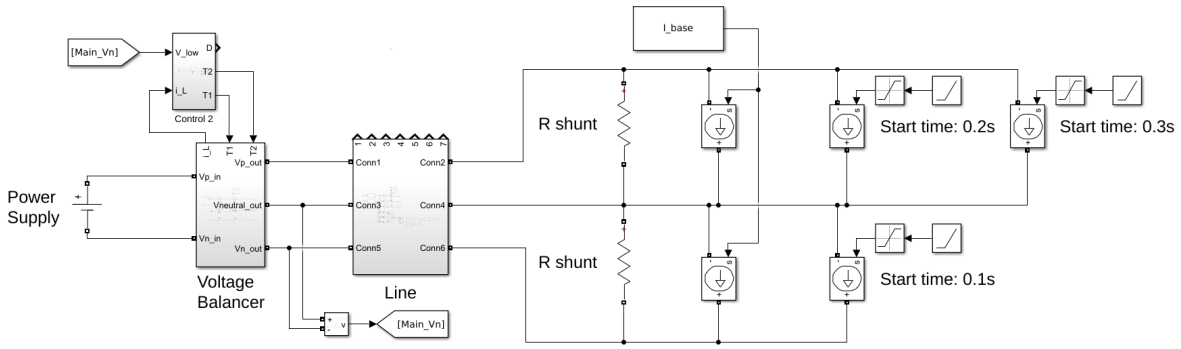

Figure 2.7: Testbench used to validate the design of the half-bridge voltage balancer

the line resistance, while the voltage of the other pole rises. The rise on the other pole is due to the voltage relationship between the two poles. Since the voltage balancer splits the power supply voltage in two, we have $V_p + V_n = V_{ref}$. Due to the action of the voltage balancer, the voltage unbalance is resorbed in aproximately 0.01 second.

Going further in the analysis, the voltage deviation caused by the changing unbalanced power of 25 kW is supposed to be of 7.5 V by design, as in Equation 2.2. Looking at Figure 2.8b, it seems that this voltage deviation is of only about 5.5 V. As the control system is rapidly taking action, it limits this change. For the third load, with a power of 50 kW, it is clear that the voltage deviation is bigger than 7.5 V. The ripple on the voltage is due to the inductor's current, itself carrying a ripple resulting from the switches, as shown previously in Figure 2.3.

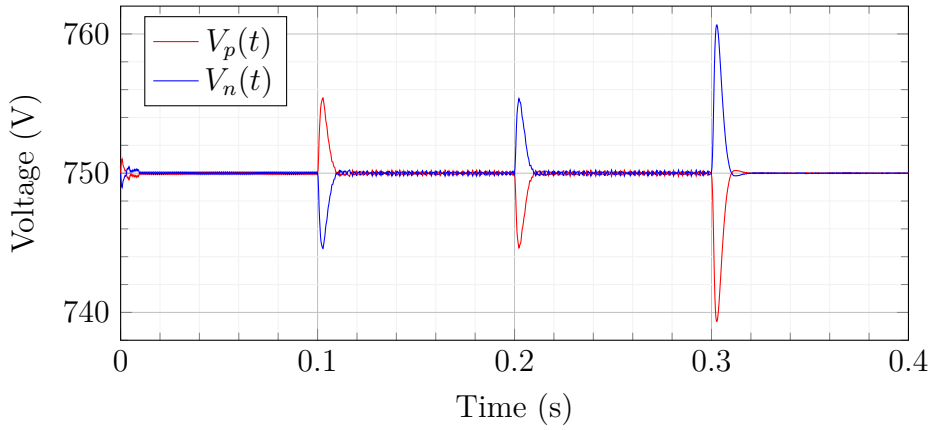

(a) Voltage balancer voltages

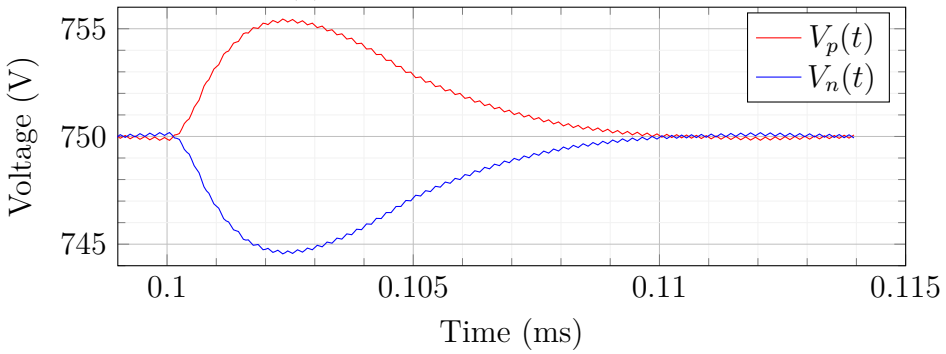

(b) Zoom on the first load turning on

Figure 2.8: Validation of the half-bridge voltage balancer design

2.2 Interleaved voltage balancer

The interleaved half-bridge voltage balancer circuit is displayed in Figure 2.9b. It is an improvement of the half-bridge voltage balancer studied in section 2.1 which is displayed in Figure 2.9a as a reminder. The main idea is to limit the current stress on

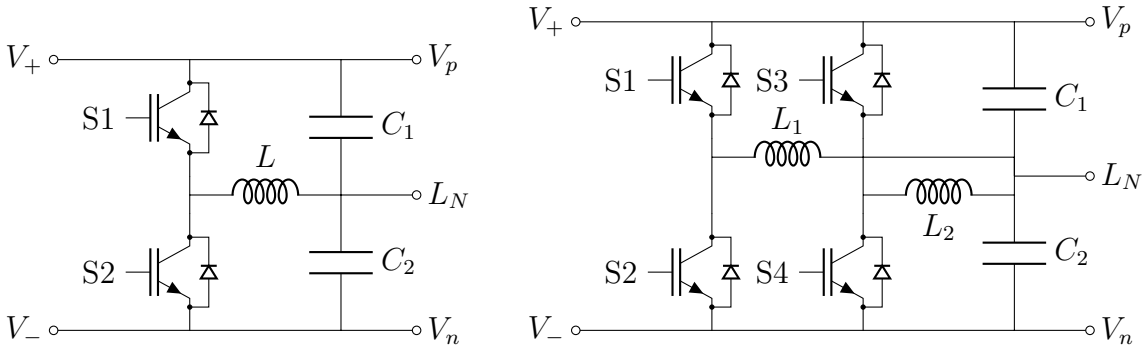

(a) Half-bridge voltage balancer (b) Interleaved half-bridge voltage balancer

Figure 2.9: Considered voltage balancer topologies

the capacitors C_1 and C_2 to maximize their lifetime and reduce losses. This improves the reliability of the voltage balancer, and thus the whole bipolar network.

This can be achieved by having multiple half-bridge branches, for which the signals applied to the gates of the switching devices are delayed by $T_{delay} = \frac{i}{N} \times T_{sw}$, with N the amount of branches, i the number of the branch from 0 to $N-1$ and T_{sw} the switching period. The sum of the current ripples in the inductors of the different branches can thus be equal to zero, and the current seen by the capacitors C_1 and C_2 is a stable DC currents in steady state.

2.2.1 Validation

The comparison of the voltages between the half-bridge voltage balancers with one and two branches are shown in Figure 2.10. In the first case (Figure 2.10a), the inductor's current $i_L(t)$ is the current as seen by the capacitors. In the second case, the current seen by the capacitors $i_{L,tot}(t)$ is the sum of the currents of both branches. As expected, the current ripple is greatly reduced, from 15 to 30 A (Figure 2.10a) down to nearly 1 A, as displayed on the zoom in Figure 2.11. Still, the total current $i_{L,tot}(t)$ is not exactly constant. It is due to the voltage balancer's control system that is continuously adapting itself, inducing small variations. The period of the currents $i_{L1}(t)$ and $i_{L2}(t)$ is equal to the switching frequency.

Regarding the voltage balancing capabilities, the comparison between the two devices is shown in Figure 2.12. Since the voltages are symmetric, only the voltages of the positive poles are displayed. As displayed, in addition to reduce the neutral current's ripple, the interleaved voltage balancer's topology can also reduce the voltage deviation when there is a sudden load variation on one of the poles. Indeed, since the voltage is more stable, the controller operating on the gates of the switching devices is more stable as well. In this case, the voltage deviation is approximately divided by 2.

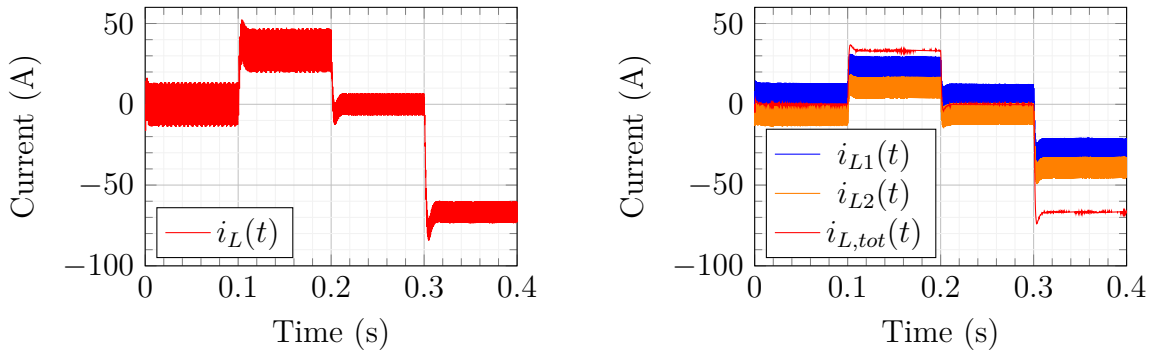

(a) Inductance current in the half-bridge voltage balancer

(b) Total current and currents in the inductances of the two-branch interleaved voltage balancer

Figure 2.10: Half-bridge and two-branch interleaved half-bridge voltage balancer's currents

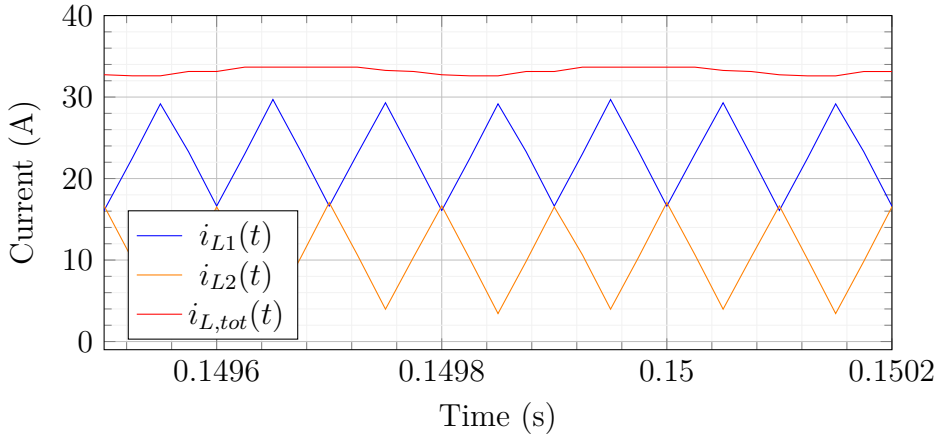

Figure 2.11: Zoom on the currents of the inductors and the total current of the two-branch interleaved voltage balancer

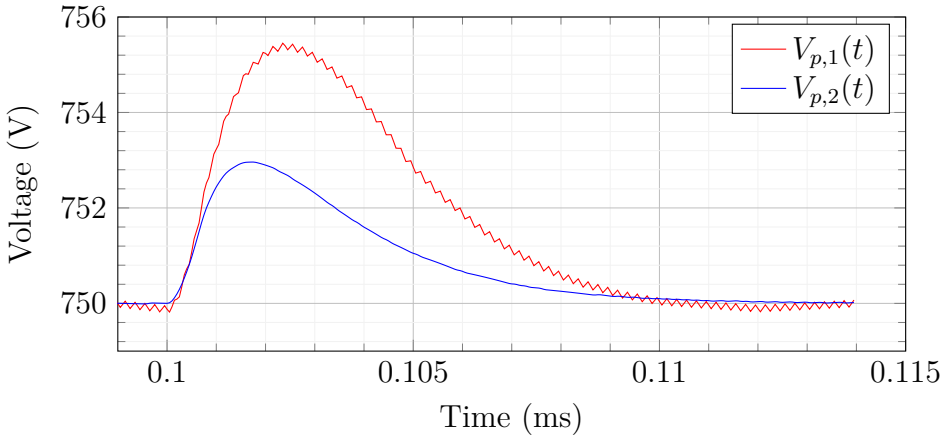

Figure 2.12: Zoom on the positive pole's voltages for the half-bridge and interleaved half-bridge voltage balancers

2.3 Standalone voltage balancer

The chosen topology for the standalone voltage balancer is the same as the previously seen half-bridge voltage balancer, with the only difference that there is no power supply connected to the standalone architecture (Figure 2.13).

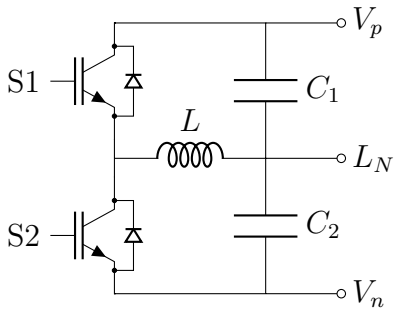

Figure 2.13: Standalone voltage balancer circuit

2.3.1 Validation

In order to validate the standalone half-bridge voltage balancer, the testbench displayed in Figure 2.14 has been used to simulate its behavior. It is the same testbench as the one used to validate the half-bridge voltage balancer (Figure 2.7), to which the standalone voltage balancer has been added. Hence, the two nodes of the network (at each side of the transmission line) are now voltage balanced.

As for the previous testbench, the first load to turn on is the negative pole at 0.1 second, L_1. Then, two loads on the positive pole turn on, L_2 and L_3. First at 0.2 second and then at 0.3 second. The powers drawn by the loads are given in Table 2.4.

In Figure 2.15, two scenarios have been compared. The first scenario corresponds to

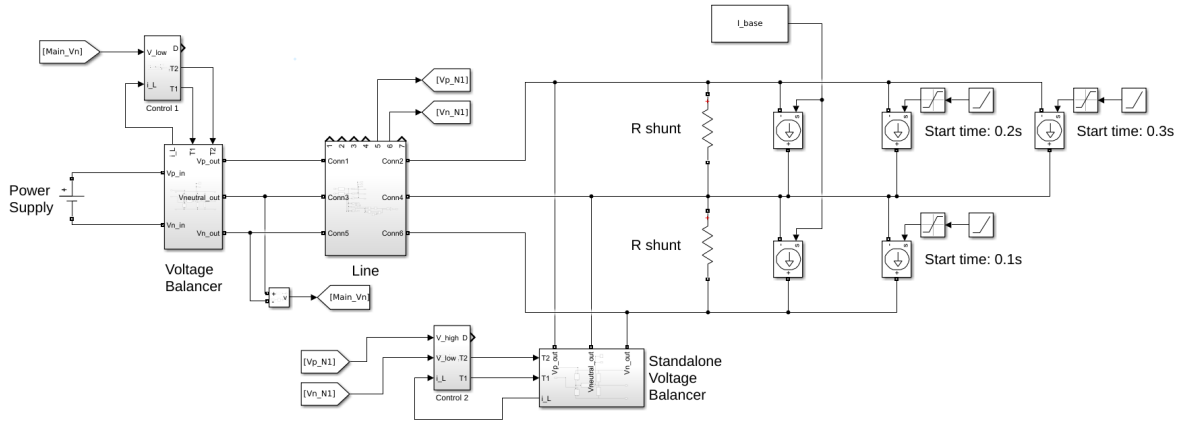

Figure 2.14: Testbench used to validate the design of the standalone half-bridge voltage balancer

Load #	Voltage [V]	Current [A]	Power [kW]	Starting time [s]
Baseload	750	133.33	100	0
1	750	33.33	25	0.1
2	750	33.33	25	0.2
3	750	66.67	50	0.3

Table 2.4: Loads power

the one described in subsection 2.1.4. In this case, there is one voltage balancer that is connected between the power supply and the DC bipolar network. For this scenario, the voltages of the two nodes (before and after the transmission lines) are displayed in Figure 2.15a and Figure 2.15b. The second scenario corresponds to the one described in this section, in which a standalone voltage balancer is added on the second node of the network. This is displayed in Figure 2.15c and Figure 2.15d, and the voltage unbalances at both nodes are cancelled as expected.

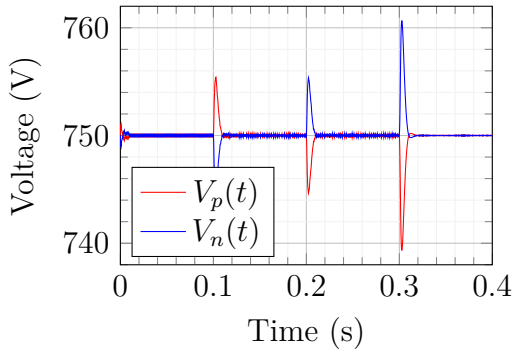

(a) Half-bridge VB: main voltages

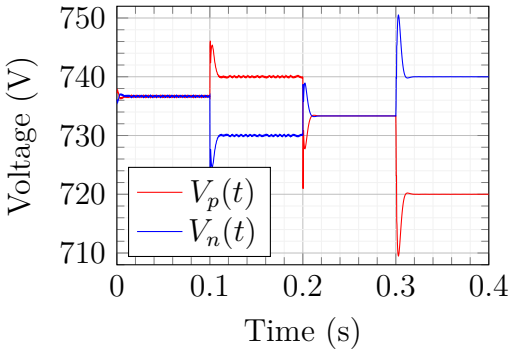

(b) Half-bridge VB: node voltages

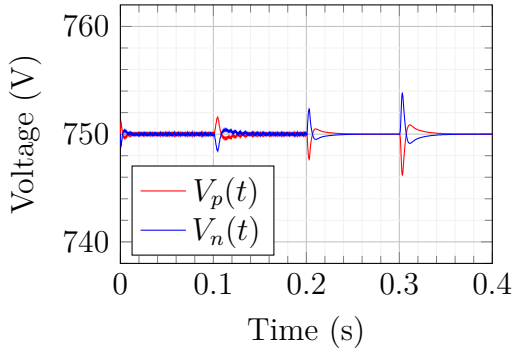

(c) Standalone half-bridge VB: main voltages

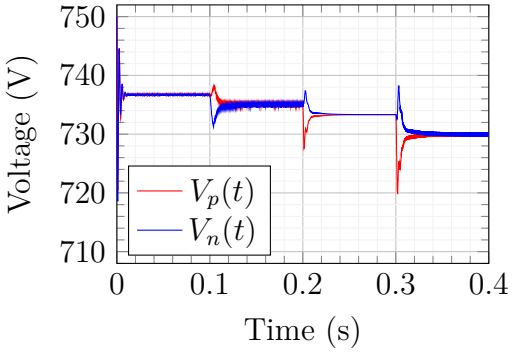

(d) Standalone half-bridge VB: node voltages

Figure 2.15: Voltages of the nodes comparison of the half-bridge VB: connected to power supply and standalone architectures

2.4 Current redistributor

As seen in subsection 1.7.3, the current redistributor circuit chosen to be used in the simulation is displayed in Figure 2.16a. The interface of this circuit is supposed to be connected somewhere in the network on the corresponding wires. The operating principle of the device is to charge the inductor with currents coming from the positive and negative wires, in order to inject it in the neutral wire. This current reinjection should be done in a way that ensures current balance, cancelling the neutral wire's current of the transmission line.

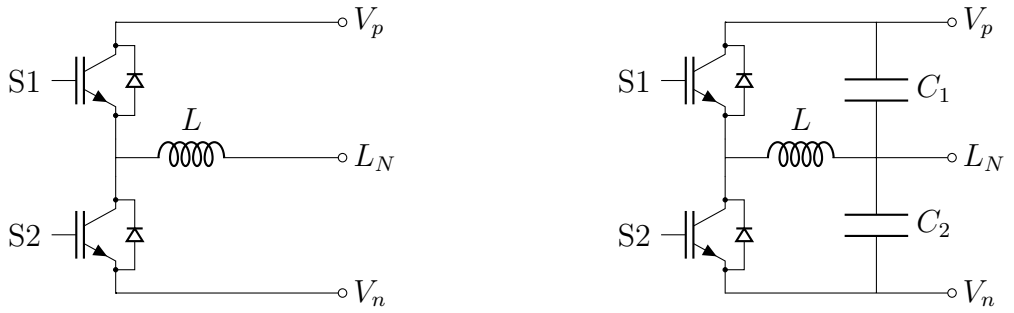

(a) CR circuit in the literature

(b) Modified CR circuit

Figure 2.16: Considered voltage balancer topologies

A current redistributor circuit used as it is would cause problems in the simulation testbench. Indeed, linking the two lines of a pole only by an inductor when the corresponding switch is closed causes voltage spikes. A solution to keep the voltages more stable is to use two capacitors, placed on each pole. This solution is the one used to keep this device usable. By doing such a modification, the modified current redistributor's circuit is the same as the half-bridge voltage balancer (Figure 2.16b). What differentiates their behavior is the control system driving the IGBTs. On one hand, the voltage balancer's control system aims to control the inductor's current to maintain the voltages of the two poles the same. On the other hand, the current redistributor's control aims to control the inductor's current in a way that it is equal to the unbalanced current to reinject (redistribute) it on the two poles.

2.4.1 Control system

Following the same principle as for the half-bridge voltage balancer (Figure 2.2), it is possible to use the same controller and remove the voltage loop. This solution is illustrated in Figure 2.17. However, since the circuit has changed due to the addition of the two capacitors, it is not possible to automatically tune the PID block using the corresponding tool in Matlab / Simulink because it doesn't represent the reality.

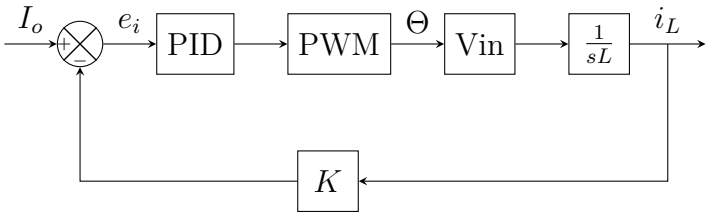

Figure 2.17: Block diagram of the control system for the current redistributor

The solution that has been used is to manually tune the PID coefficients by trial and errors to obtain the desired response. In order to keep the tuning as simple as possible, the method is to begin with the proportional coefficient K_p, then the integral coefficient K_i, and if needed the derivative coefficient K_d.

2.4.2 Components

The components used for the current redistributor's circuit are the same as for the half-bridge voltage balancer. Although the choice for the switching devices is the same (IGBTs), the capacitors and the inductance values are not.

The sizing of the inductor follows the same idea as for the voltage balancer's inductor. Theoritically, the same size of inductor could be taken. That would be possible if the control system was as good as for the voltage balancer. Indeed, as explained further in chapter 4, the PID coefficients found for the control system induce bigger oscillations, that can be seen on the voltages of the poles, and it degrades the overall stability. In order to limit the ripple of the inductor's current, tripling the inductor's size showed to be effective.

Regarding the capacitors, there is no need to keep them as big as the ones used for the different voltage balancers discussed earlier. Indeed, for those circuits, their size is chosen to limit the voltage deviation when there is a sudden change of power drawn by the loads that modifies the unbalance situation. On the other hand, a current redistributor doesn't aim to balance voltage. In the situation described in this paper, a value of 0.7 mF, which is about a third of the corresponding components for the voltage balancers, showed to be effective enough to obtain the expected behavior of the circuit. The value of the parameters used for the current redistributor are summarized in Table 2.5.

2.4.3 Validation

The testbench used to validate the behavior of the studied current redistributor is displayed in Figure 2.18. The voltage balancer used as a connection point between

Parameter	Value	Unit
f_{sw}	10	kHz
L	8.43	mH
C	700	μF

Table 2.5: Sumary of the current redistributor's paramaters

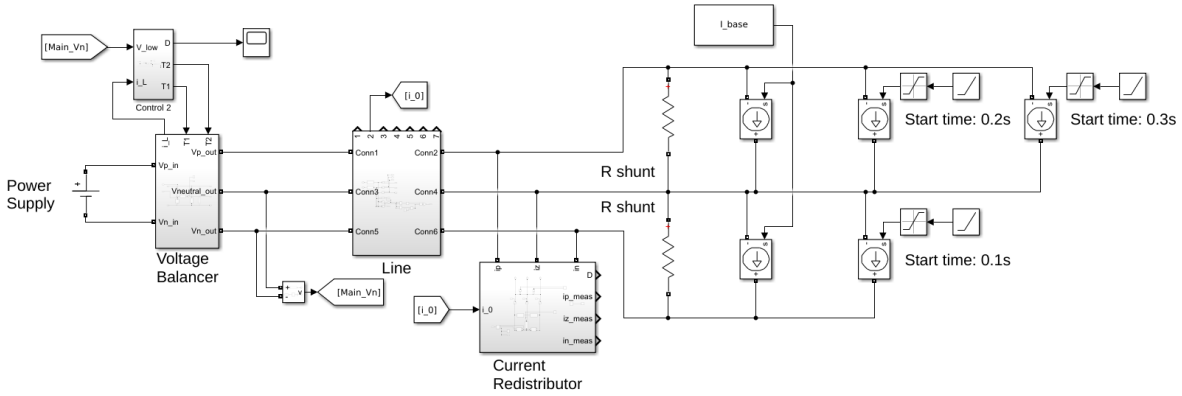

Figure 2.18: Testbench used to validate the current redistributor

the unipolar power supply and the bipolar network is the half-bridge voltage balancer discussed in section 2.1. The reference current provided to the current redistributor control system is the neutral wire's current of the transmission line. In other words, the current redistributor control system aims at maintaining this current to zero. The loads behavior is the same as seen before, with a summary given in Table 2.4. The currents drawn by the loads and flowing through the transmission line is represented in Figure 2.19a.

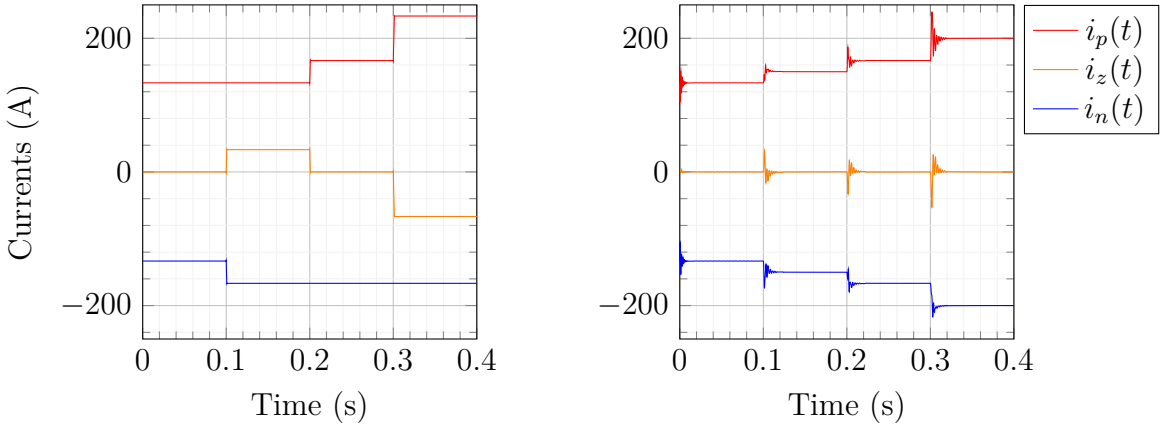

(a) Line currents without a current redistributor

(b) Line currents when using the current redistributor

Figure 2.19: Line's currents comparison with and without the use of a current redistributor

For this system, only using a PI controller gives acceptable results to prove that the circuit is working. The device's current behavior is displayed in Figure 2.19b. As expected, the neutral wire's current is kept equal to zero thanks to the device's action.

2.5 Precharge circuit

The previous sections of this chapter described the behavior of the different voltage balancers and the current redistributor studied in a small testbench to validate their behavior. Some topologies are specifically designed and thought to be used like a *plug and play* solution, like the standalone voltage balancer or the current redistributor, meaning that they can connect at any node and they don't need to be connected to a power supply. As seen in Figure 2.15b for the voltages (between 0.2s and 0.3s) and in Figure 2.19b for the currents (between 0s and 0.1s), in some cases the system is balanced at a specific node and connecting such devices might not be necessary. In such scenarios, the relatively significant drawback of the internal losses of the devices might lead to a desire to disconnect them.

If this is the case, a precharge circuit is needed, both for the standalone voltage balancer and the current redistributor. Indeed, since capacitors are present between the two poles, the voltage differences between the voltages of the network's poles and the standalone device's poles create in-rush currents. This is true if the connection method is using simple switches. Doing so might also extend their lifetime.

A precharge circuit is a circuit located between the device to be connected and the network it connects to. It consists of two paralel subcircuits: the first one is a switch in series with a resistor, and the second one is made of a single simple switch [33]. The circuit is shown in Figure 2.20. The operating principle is as follows: first, the switch S_1 closes, linking the terminals n_1 and n_2 by the resistor R. Knowing the voltage difference between the two terminals, it is possible to size the resistor in a way that limits the in-rush current to a chosen value. This is done by applying Ohm's law $\Delta U = R \times I$. Rapidly, the in-rush current decreases because the capacitors are now charged. Once this is the case, the switch S_2 can be closed, and the switch S_1 opened. The two interfaces are now connected without any resistors, and the circuit can operate as designed on the network.

In order to validate the behavior of this circuit, it is tested on the current redistributor described and tested in section 2.4. For simplicity and to keep the simulation fast enough so that graphs are easy to read, it is assumed that the capacitors of the device to be connected are maintained at a voltage of 300 V. Since the voltage of the network's poles is 750 V, that means that the voltage difference between the two is of 450 V.

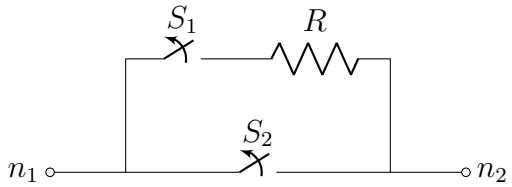

Figure 2.20: Precharge circuit implementation between the node n_1 and n_2

It can also be assumed that the in-rush current has to be limited to at most 100 A. Following Ohm's law in Equation 2.17, the value of the resistor has to be equal to $R = 450V/100A = 4.5\Omega$.

$$\Delta U = R \times I \tag{2.16}$$

$$R = \frac{\Delta U}{I} \tag{2.17}$$

Knowing that the energy stored in a capacitor when charged by a resistor is proportional to its charge given by

$$Q = CV(1 - e^{-t/\tau}) \tag{2.18}$$

where Q is the charge stored in the capacitor in Coulomb, C its value in Farad, V the charging voltage in Volt and $\tau = R \times C$ its time contant in second with R the resistor in Ω charging the capacitor. It can be assumed that disconnecting the precharge branch and connecting directly the capacitor to the network is acceptable if it is charged up to 95% of its capacity, then it is possible to obtain the precharge time. Indeed, from Equation 2.18 we have

$$1 - e^{-t/\tau} = 0.95 \tag{2.19}$$

$$e^{-t/\tau} = 0.05 \tag{2.20}$$

$$\frac{-t}{\tau} = ln\,0.05 \tag{2.21}$$

$$t = -\tau \times ln\,0.05 \tag{2.22}$$

$$t = -RC \times ln\,0.05 \tag{2.23}$$

$$t \simeq 3 \times RC \tag{2.24}$$

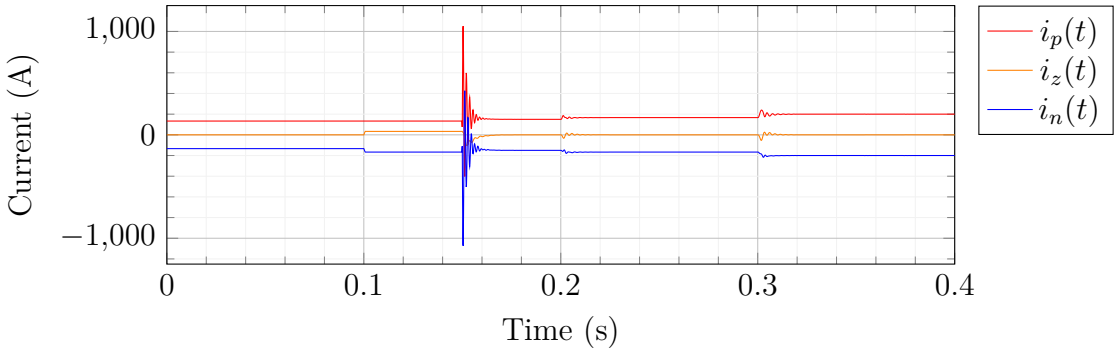

(a) Line currents without the precharge circuit connected the current redistributor

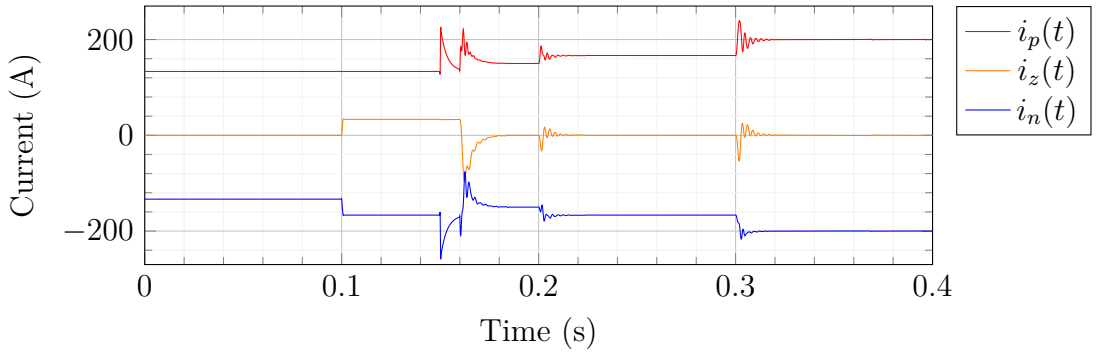

(b) Line currents with the precharge circuit connected the current redistributor

Figure 2.21: Line's currents comparison when connecting the current redistributor with and without a precharge circuit

From Equation 2.24 and the values $C = 0.7 \times 10^{-3}$ F and $R = 4.5\,\Omega$, we find $t = 9.45 \times 10^{-3}$ s. In the simulation, the value $t = 10$ ms has been used.

To compare the behavior of the circuit with and without a precharge circuit, Figure 2.21 displays the transmission line's currents for both cases, when the current redistributor is connected at 0.15s to the network. What can be seen in Figure 2.21a is that the in-rush currents can be quite large relatively to the nominal currents flowing in the cables. On the other hand, with the precharge circuit, the in-rush currents are limited to approximately 100 A, as wished when desgining this circuit. This corresponds to the currents seen at 0.15s. After 10ms, the second current spikes are due to the control system's oscillations. After the current's variations due to the connection, both scenarios behave identically.

Chapter 3

Methodology

This section describes the methodology used to assess the performances of the devices discussed in the previous chapter. Indeed, in chapter 2, the focus was solely on designing and verifying if the studied devices functioned as expected. The next step is to place them in a test network to assess how they interact in a slightly more complex network, that could better represent what is done in the industry.

Regarding the simulations, they will be performed with the Simulink simulation tool of Matlab, as in chapter 2.

3.1 Testbench

The testbench used to represent the microgrid is composed of a main DC unipolar power supply connected to a voltage balancer creating the DC bipolar network. From there, two radial branches radiate and are composed respectively of two and three nodes. Each node is connected to the other with a RL transmission line. With the node connecting the two branches, the network is made of six nodes. This is summarized in the diagram of Figure 3.1. This configuration is interesting because by placing a device on the fifth node for example, it is possible to evaluate its impact on the two adjacent nodes as well as the nodes on the other branch.

The design choices for the lines, the power supply as well as the load profiles are described in the following subsections. As explained previously, the network tends to represent a network providing access to electricity in an industrial area. The design assumes that the total length of the network from node 3 to node 6 is 1 kilometer, meaning that each line is 200 meters long. The complete Matlab / Simuling implementation of the testbench is described in Appendix B.

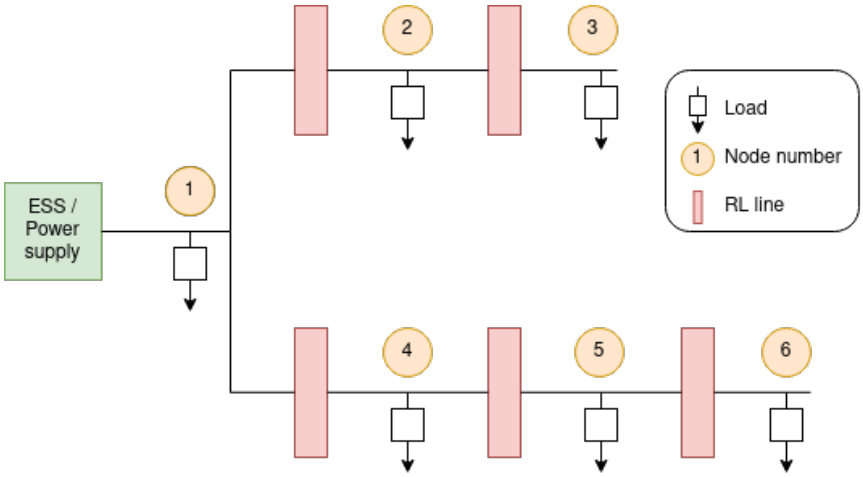

Figure 3.1: First design of the testbench

3.1.1 Lines

Each line is represented as a three wire RL impedance. The line resistance coincides with the physical resistance of the cable, while the inductance is required to simulate the length of the cable during transient operation. The value per unit of length for the resistance and inductance are chosen arbitrarily in a range that would make sense for the network. The main goal is to show the interaction between the voltage balancers and current redistributor and the grid, and not to model perfectly the grid and its losses. The chosen values are displayed in Table 3.1.

Symbol	Per length	Value	Description
L_{line}	10^{-6} H/m	10^{-4} H	Inductance of the line
R_{line}	$0.5^{-3}\,\Omega$/m	$0.1\,\Omega$	Resistance of the line

Table 3.1: RL impedance of the 200m long lines

3.1.2 Power supply

The power supply of the network is an unipolar DC ideal source. It is connected to the main voltage balancer. The chosen voltage balancer's topology is the half-bridge, discussed in section 2.1. Indeed, it is the simplest and cheapest one. The voltage provided by the power supply is 1500V, which is equally split between the two poles.

3.1.3 Loads

The load profiles come from the data discussed in Appendix C. The baseload powers are summarized in Table 3.2, while the varying load profiles are summarized in Table 3.3.

Node	Power	Voltage	Current
1	50 kW	1500 V	33.33 A
2	40 kW	1500 V	26.67 A
3	40 kW	1500 V	26.67 A
4	40 kW	1500 V	26.67 A
5	20 kW	1500 V	13.33 A
6	10 kW	1500 V	6.67 A

Table 3.2: Baseloads power, voltage and current

Node	Pole	Power	Voltage	Current	Starting time
5	V_n	12.5 kW	750 V	16.67 A	0.1 s
6	V_n	25 kW	750 V	33.33 A	0.2 s

Table 3.3: Varying loads power, voltage and current

3.2 Scenarios

In order to assess the impact of voltage balancing and current redistributing on the network, four different scenarios are simulated and discussed. The first one corresponds to a simulation of the testbench as it is, with only the main voltage balancer at node 1. The goal is to have a base case for comparison. The second one is the same but includes a standalone voltage balancer at node 5. The idea is to be able to assess if this additional device can mitigate the voltage unbalance, and see its effect on the other nodes. The third one is the same as the first, but includes a current redistributor at node 6. That way, it is possible to monitor how the current balancing influences the voltages and the losses. Finally, the last scenario will include both the standalone voltage balancer at node 5 and the current redistributor at node 6 to see how they interact. A summary of the different simulation scenarios is given in Table 3.4.

Scenario #	Main VB	Standalone VB	CR	Point of connection
1	Half-bridge	-	-	-
2	Half-bridge	Half-bridge	-	Node 5
3	Half-bridge	-	Half-bridge	Node 6
4	Half-bridge	Half-bridge	Half-bridge	Node 5 / Node 6

Table 3.4: Simulation scenarios: devices used and point of connection

3.3 Criteria to evaluate performances

Evaluating performance is done through the use of different criteria. Here, they will be presented so they can be used in the simulations. The formula defining those criteria are based on the sign conventions used in Figure 3.2.

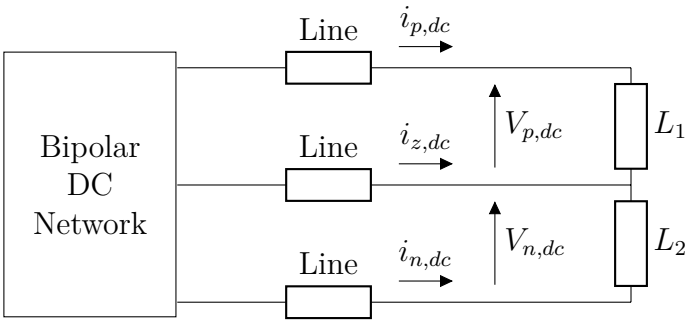

Figure 3.2: Simple representation of a bipolar DC network showing the sign convention for the voltages of the poles and the currents of the lines

3.3.1 Line Voltage Unbalance Rate

The line voltage unbalance rate for a bipolar DC network (%LVUR$_{DC}$) is defined as the voltage magnitude deviation of the positive and negative pole divided by the average voltage magnitude of the poles, as shown in Equation 3.1 [15] [34]. This formula is based on the voltage unbalance rate in an AC system [35].

$$\%\text{LVUR}_{DC} = \frac{|V_{p,dc} - V_{n,dc}|}{(V_{p,dc} + V_{n,dc})/2} \times 100 \ \ [\%] \tag{3.1}$$

3.3.2 Line Current Unbalance Rate

Following the same idea as for the %LVUR$_{DC}$, this thesis presents a new way of assessing the current unbalance rate in bipolar DC networks, named %LCUR$_{DC}$. The idea is to give in percentage the difference between the positive wire's current and the negative wire's current compared to the average of those currents. In other words, it corresponds to the neutral wire's current divided by the average of the magnitude of two other currents. The corresponding formula is given by Equation 3.2.

$$\%\text{LCUR}_{DC} = \frac{|i_{p,dc} + i_{n,dc}|}{(i_{p,dc} - i_{n,dc})/2} \times 100 = \frac{|i_{z,dc}|}{(i_{p,dc} - i_{n,dc})/2} \times 100 \ \ [\%] \tag{3.2}$$

3.4 Assumptions and limitations

In any research project, it is necessary and essential to evaluate its assumptions and limitations that may impact the presented results. Throughout this section, those limitations are listed, explained and grouped in different categories.

This section's importance is even greater knowing that the literature on bipolar DC microgrid is scarce. By providing a transparent and comprehensive list of assumptions and limitations, future researchs can be built upon this knowledge and be more accurate.

Model simplifications: In this network, the loads present on the microgrid are modeled as ideal constant current sources. Changing the consumed power of the load is done by increasing the drawn current with a slope of 5×10^4 A/s. The internal losses of the studied devices are not taken into account. The only exception is for the IGBTs, where the conduction losses are taken into account through a small conduction resistance. The temperature behavior of the components are not taken into account, so any temperature-induced variation is not represented in this work.

Control system assumptions: The transmission time between the measurements of the input voltages and currents and the control system is instantaneous. The propagation time of the signal from the input to the output of the control system is also zero. In real-world applications, the propagation time of the measurements and control systems chains might induce different behaviors.

Simulation scenarios: The studied possibilities are rather limited. Four different scenarios are discussed, within a very short timeframe of 300ms. Since there are only two load connections for each scenarios, 8 different reactions are tested on a small portion of the network (node 5 and node 6).

Scalability and generalization: Resulting from the limitations of the simulation scenarios, the studied model lacks possibility of scalability and generalization. Only one radial network architecture with one power supply and two branches is studied. In reality, networks can have loop configuration, longer lines, loads with different behavior, to name but a few. Lots of possibilities exist that could not be taken into account in this thesis.

Software limitations: As explained in section 1.5, the shoot-through problem can be avoided by changing the charging and discharging time of the gate capacitor of the switching devices. Unfortunately, Simulink provides natively only MOSFETs and

IGBTs based on ideal switches. It is thus more complex to recreate conditions that would lead to this issue.

Security and faulty operation of the system: No security analysis has been performed. No faulty behavior of the network was simulated.

Chapter 4

Presentation and discussion of the simulation results

This chapter presents the simulation results obtained from the scenarios described in chapter 3. As mentioned in section 3.2, the simulation scenarios are displayed again in Table 4.1. Once the results are described, section 4.5 opens a discussion about where to place voltage balancers and current redistributors in a bipolar DC microgrid, answering the fourth research question of this thesis.

Throughout the presentation of the simulation results, the voltages are first fully displayed in Volts, to be gradually replaced by a measure of the LVUR_{DC}. Indeed, once the general behavior of the voltages is understood, it is easier to measure the voltage deviations using LVUR_{DC}. The same holds true for the current distributions and the LCUR_{DC}.

Scenario #	Main VB	Standalone VB	CR	Point of connection
1	Half-bridge	-	-	-
2	Half-bridge	Half-bridge	-	Node 5
3	Half-bridge	-	Half-bridge	Node 6
4	Half-bridge	Half-bridge	Half-bridge	Node 5 / Node 6

Table 4.1: Reminder of the simulation scenarios: devices used and point of connection

4.1 First scenario

The first scenario corresponds to a network in which no balancing device is present, except the main voltage balancer, being the interface between the unipolar DC power

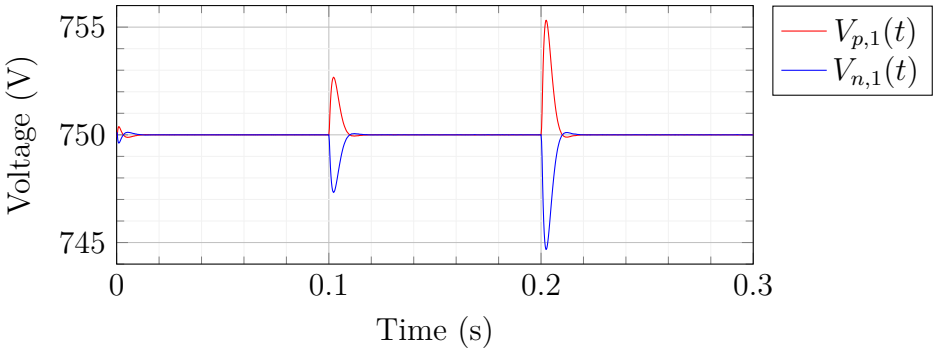

Figure 4.1: Scenario 1 – Node 1 voltages

supply and the bipolar DC microgrid. Since the power in the network is balanced at the beginning of the simulation, and the power unbalances arise at node 5 at 0.1s and at node 6 at 0.2s, the line currents are balanced in the upper branch of the network (node 2 and 3), while the currents in the lower branch of the network are not (node 4, 5 and 6). The currents flowing at the bipolar interface of the main VB are thus not balanced and it is expected to see a balancing reaction to maintain the voltage balance at node 1 around 0.1s and 0.2s. This behavior of the voltage balancer is displayed in Figure 4.1. For a power deviation of 25 kW (at 0.2s), the corresponding voltage deviation is of approximately 5.5 V, which is the same as what was observed while validating the behavior of the circuit in subsection 2.1.4.

Considering the upper branch, since the currents in the positive and negative wires are exactly opposite, the voltage drops accross the transmission lines are equal. In this case, if the voltage balance is perfect, meaning that the $\text{LVUR}_{DC} = 0\%$, then the voltages after the transmission lines are balanced as well. Following this idea, if the voltage upstream of a transmission line changes, but the current stays the same, then the voltage drop after the transmission line is proportional to the upstream voltage deviation. This follows Ohm's law with $\Delta U = R \times I$. So when the power distribution changes and the main voltage balancer acts on the voltages at node 1, then the downstream branch made of the nodes 2 and 3 experiences the same voltage deviation. This can be seen for both nodes in Figure 4.2a and Figure 4.2b. The voltage levels of node 3 are lower than for node 2 because the total resistance of the lines between node 3 and node 1 is higher than between node 2 and node 1. This comes from the lengths of the lines.

To see how the unbalance propagates from node 1 to nodes 2 and 3, the measurements of the LVUR_{DC} at those nodes is shown in Figure 4.2c. Even though it seems like there is only one curve, it is not the case. The LVUR_{DC} are so close that they are on top of each other. A first observation is that the LVUR_{DC} is maintained on a balanced branch of the network, propagating from the most upstream node to the end node.

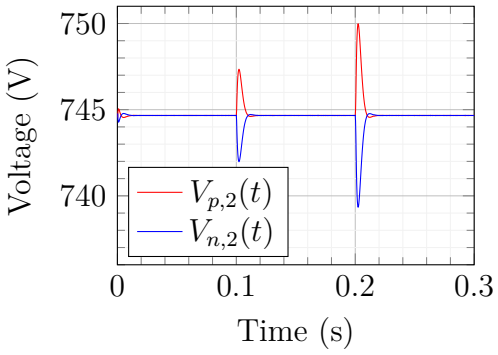

(a) Scenario 1 – Node 2 voltages

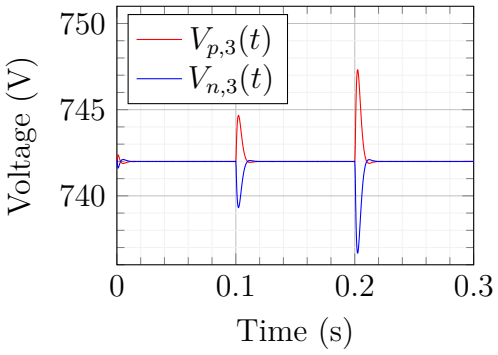

(b) Scenario 1 – Node 3 voltages

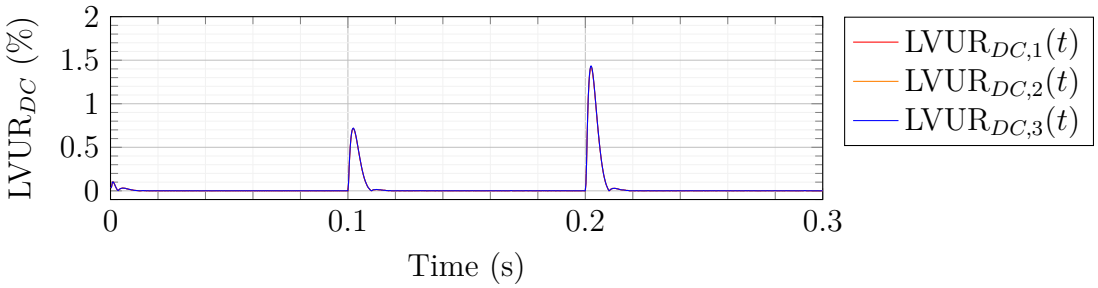

(c) Scenario 1 – LVUR_{DC} of node 1, 2 and 3. The curves are so close that it looks like there is only one curve

Figure 4.2: Scenario 1 – Comparison of the voltages of node 2 and node 3

The focus is now on the lower branch, the one that contains the nodes 5 and 6 where unbalances arise. The analysis of the voltages and the LVUR_{DC} at the different nodes are done in three different steps, for three different timesteps of the simulation. The currents flowing through the transmission lines between each node are displayed in Figure 4.3.

Between 0 and 0.1 second, the whole branch is balanced, from node 1 to node 6. Since the currents in the positive and negative wires are equal in magnitude, the neutral wire's current is equal to zero. This leads to no voltage drop on the neutral wire, and

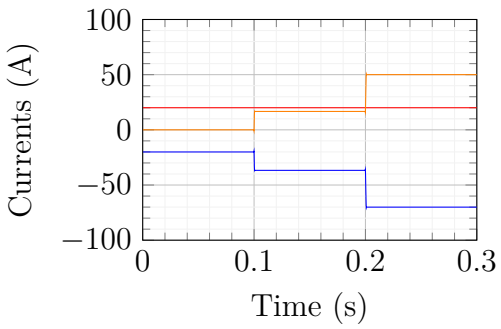

(a) Line currents at node 5

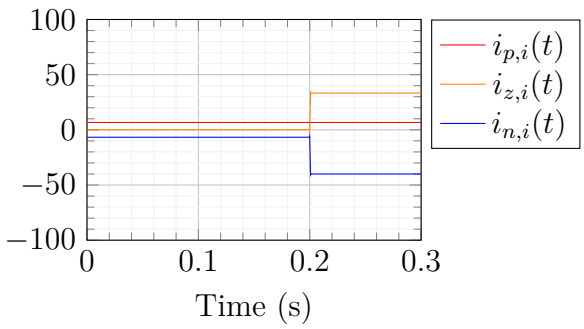

(b) Line currents at node 6

Figure 4.3: Scenario 1 – Line currents at node 5 and node 6

equal voltage drops accross the transmission lines on the positive and negative poles. So even if the voltage levels are lower at node 5 (Figure 4.4a) and 6 (Figure 4.4b) compared to node 1 due to the resistance of the line, they are still equal for both poles. It follows that $\text{LVUR}_{DC,4} = \text{LVUR}_{DC,5} = \text{LVUR}_{DC,6} = 0$ for nodes 4, 5 and 6, as see in Figure 4.4c.

Between 0.1 and 0.2 second, a load connects on the negative pole at node 5, creating an unbalance of 12.5 kW. This unbalance leads to different currents flowing in the wires, all the way from node 1, where the power supply is connected, to node 5. This creates different voltage drops along the lines, leading to different pole voltages and a non-zero LVUR_{DC}. Since the lines are longer from node 1 to node 5 compared to node 4, we have that $\text{LVUR}_{DC,5} > \text{LVUR}_{DC,4}$. Also, since the line currents flowing from node 5 to node 6 are the same, the LVUR_{DC} is maintained between those two nodes, for the same reason as it was the case for the upper branch of the microgrid.

Finally, between 0.2 and 0.3 second, the last load connects on the negative pole of node 6. The additional current feeding this load flows all the way from the power supply to node 6, increasing the overall currents, the voltage drops accross the lines and thus the LVUR_{DC}. In this timestep, the loads connected at node 6 are not balanced anymore, and the unbalance is expected to increase between node 5 and node 6, leading to $\text{LVUR}_{DC,6}$ becoming bigger than $\text{LVUR}_{DC,5}$ at 0.2s.

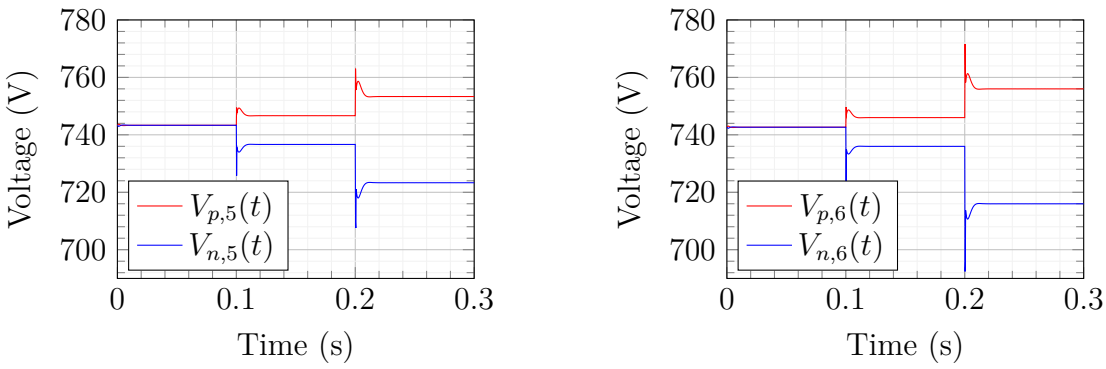

(a) Scenario 1 – Node 5 voltages

(b) Scenario 1 – Node 6 voltages

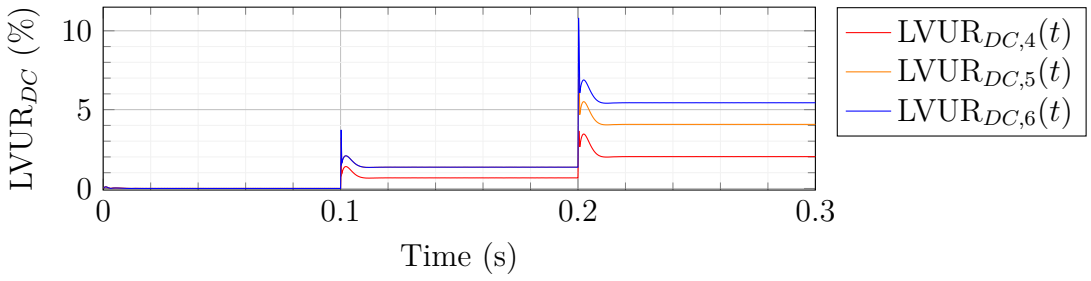

(c) Scenario 1 – LVUR_{DC} of node 4, 5 and 6

Figure 4.4: Scenario 1 – Comparison of the voltages of node 5 and node 6

4.2 Second scenario

The second scenario takes the first one as base, and includes an additional standalone voltage balancer connected at node 5. The loads profiles are unchanged. Voltage levels at nodes 5 and 6, as well as the LVUR_{DC} of nodes 4, 5 and 6, are displayed in Figure 4.5.

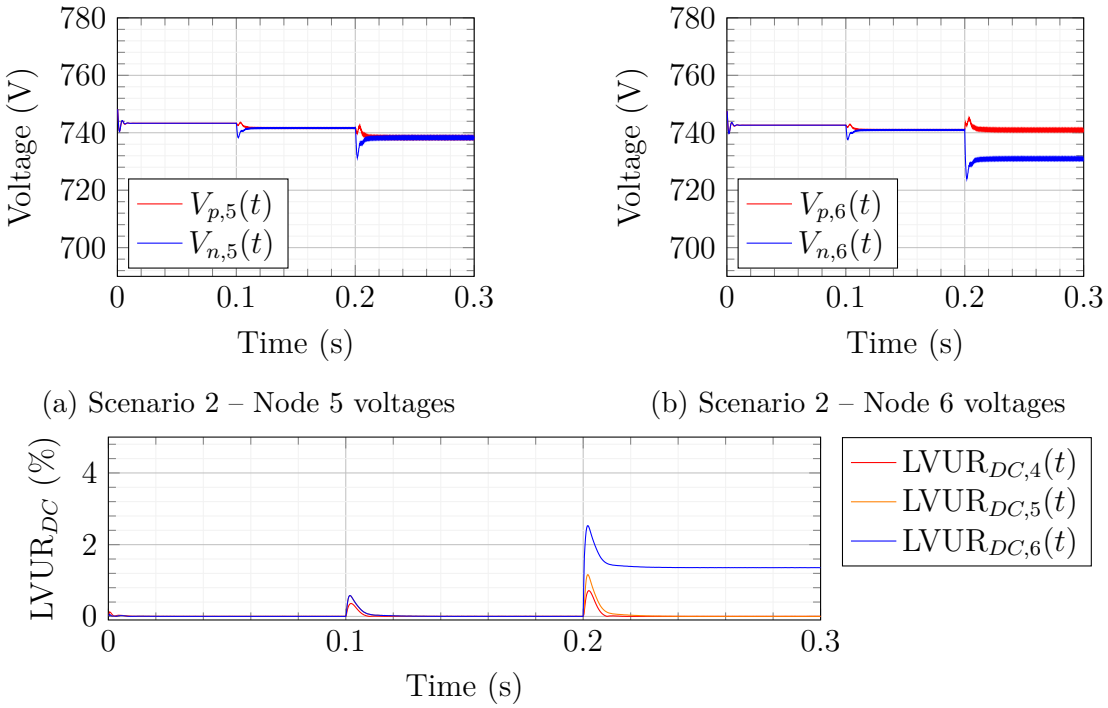

(a) Scenario 2 – Node 5 voltages

(b) Scenario 2 – Node 6 voltages

(c) Scenario 2 – LVUR_{DC} of node 4, 5 and 6

Figure 4.5: Scenario 2 – Comparison of the voltages of node 5 and node 6

What is interesting to notice is that in this case, the voltages of both poles are kept balanced at node 5 thanks to the action of the standalone voltage balancer, as it can be seen in Figure 4.5a. Since the downstream node, node 6, has its power balanced until 0.2s, and that the upstream node, node 5, has now its voltages balanced, the unbalance that was present in the previous scenario between 0.1s and 0.2s (Figure 4.4c) is not present anymore, as it can be seen in Figure 4.5c.

Furthermore, as seen in the previous scenario, the unbalance at node 6 due to the unbalanced load turning on at 0.2s is adding to the propagating unbalance coming from the upstream nodes. With node 5 voltages being balanced with the action of the newly added standalone voltage balancer, only the unbalanced loads of node 6 are responsible for the value of the LVUR_{DC} at its node (Figure 4.5c). This lead to a lower value compared to the first scenario.

Regarding the voltage levels at node 1, the corresponding LVUR_{DC} is expected to be lower since the unbalances are taken care of between the main voltage balancer of

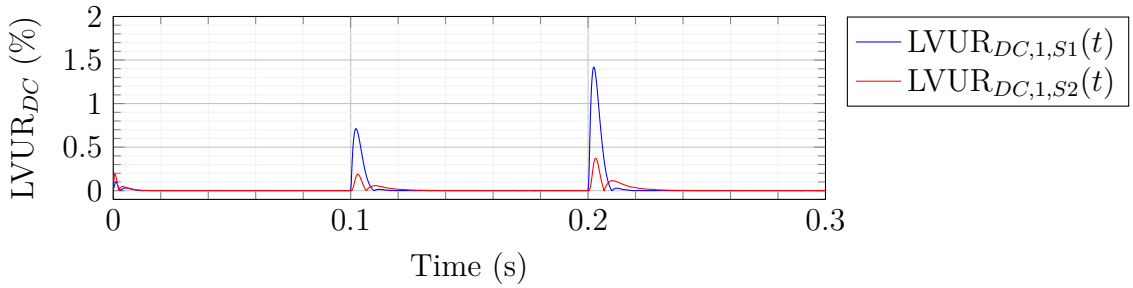

Figure 4.6: Comparaison of the LVUR$_{DC}$ of the first node, for the first (S1) and second (S2) scenarios

node 1 and the nodes causing them. Theoretically, as seen from node 1, the network is balanced thanks to the action of the newly added device. This can be seen in Figure 4.6. The variation occuring at the loads activation time is due to the voltage balancers adjusting to the new power distribution through the action of the control system.

4.3 Third scenario

The third scenario takes the first one as base, and includes an additional current redistributor connected at node 6. It is assumed that the device is automatically connected when the LCUR$_{DC,6}$ reaches a threshold set by the grid maintainer. In this case, the load connecting at 0.2s on the negative pole triggers the turn on of the device after 10ms, at 0.21s. The precharge circuit is on for a duration of 10ms as in section 2.5.

This can be seen in Figure 4.7b. For comparison purposes, the corresponding line currents for the first scenario (without the current redistributor) are displayed in Figure 4.7a. The first current peak happening at 0.21sin Figure 4.7b is due to the precharge circuit charging the capacitor. At this point, the control system of the current redistributor is not active yet. At 0.22s, the connection between the device and the grid is made, and the resistors of the precharge circuit are disconnected. The control system begins to operate, and oscillates for approximately 30ms before being stable. After those 40ms of total connection time, the currents are balanced as expected. The LCUR$_{DC}$ of this node for both scenarios are displayed in Figure 4.7c. As it can be seen, the currents are balanced around 0.25s. The spikes displayed between the interval 0.22s and 0.23s are due to the oscillation of the control system, causing the denominator of Equation 3.2 to be close to zero, leading to very high values.

As explained in section 1.1, the line losses are minimal when $i_p = i_n$. Any other currents distribution leads to additional losses on the network's lines. Figure 4.8 displays the line losses between nodes 5 and 6. Since the baseload is relatively small compared to the load turning on at 0.2s, the losses are rather small before. Between 0.2s and

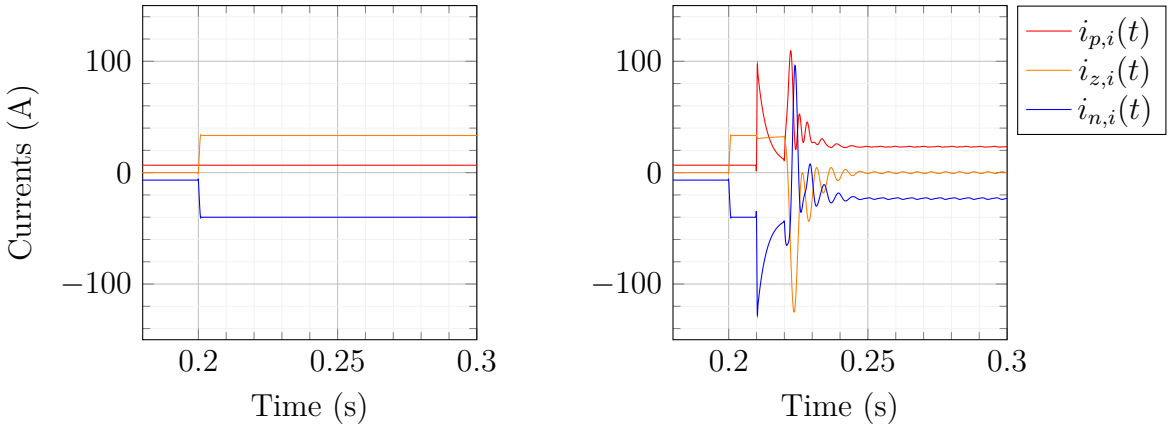

(a) Scenario 1 – Line currents at node 6

(b) Scenario 3 – Line currents at node 6

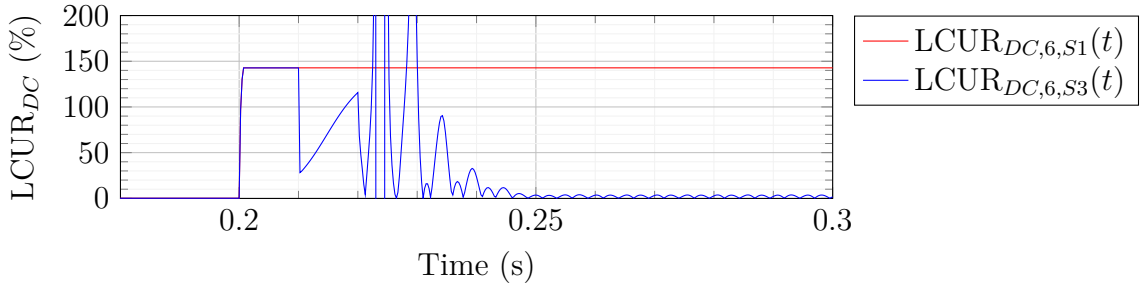

(c) Scenario 2 – LCUR_{DC} of node 6 for the first (S1) and third (S3) scenarios

Figure 4.7: Comparison of the line currents at node 6 for scenarios 1 and 3

0.21s, the non-optimal losses are the result of non-balanced currents in the lines. The next 10ms correspond to the precharge circuit connecting the device with the network, and the following 30ms correspond to the oscillation of the control system on its way to stabilize the currents. At 0.25s in the simulation, the control system is stable and the circuit is again at steady state. As expected, the line losses are now lower, by approximately 40% on this example.

Concerning the two loss spikes in the graph of Figure 4.8, solutions can be implemented to limit them if it is considered as too much to handle for the grid. The first spike is due to the currents charging the capacitors of the current redistributor through the precharge circuit. As explained in section 2.5, the magnitude of the charging currents is determined by the size of the resistor. At the expense of the charging time, those in-rush currents can be kept relatively low simply by increasing the connecting resistance. The second high instantaneous power loss is due to the oscillation of the current redistributor's controller. Indeed, as explained in subsection 2.4.1, the PI controller's coefficients have been chosen by trials and errors. This means that there is no guarantee that they are optimal, and chances are they are far from the best values for this application. Using a more robust approach to design the control system of the current redistributor is believed to give a better transient behavior, leading to less

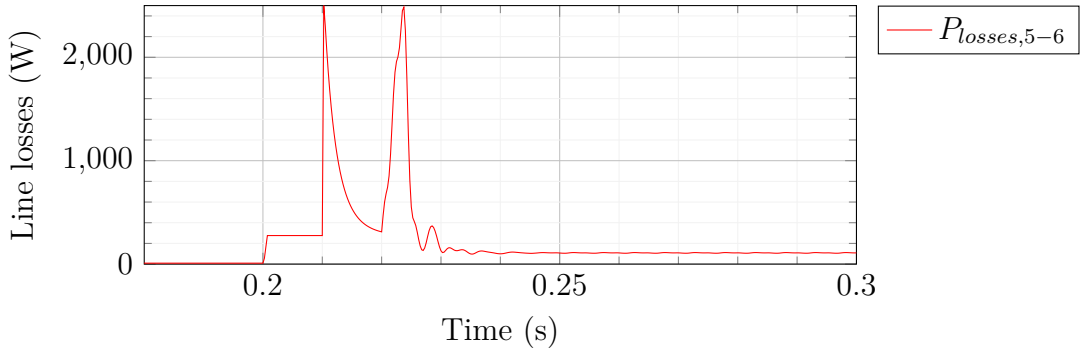

Figure 4.8: Scenario 3 – Line losses between nodes 5 and 6

current oscillations and thus limiting the corresponding line losses.

Regarding the impact on the voltages, they are displayed for nodes 1 and 6 in Figure 4.9. The relatively high currents oscillations due to the control system of the current redistributor have a direct proportional impact on the voltages of the nodes. Those voltage levels for nodes 5 and 6 are displayed in Figure 4.9a and Figure 4.9b. The LVUR_{DC} for the bottom branch of the network, with nodes 4, 5 and 6, are displayed in Figure 4.9c. Again, it can be observed that between 0.2s and 0.22s, before the control system operates, the voltage unbalance is getting higher the more it is far away from the main power supply. Indeed, the voltage drops on the line due to the current distribution is proportional to the resistance of the lines, getting higher with the distance. The same explanation holds while the control system oscillated until it is stable. Once it is stable, approximately at 0.25s, then the voltage unbalance levels for nodes 4, 5 and 6 are the same as before the load turned on. Thanks to the current redistributor's action, the voltage drops on the lines between nodes 5 and 6 are the same for both poles, maintaining the LVUR_{DC} for those nodes equal.

At this point, the effect of adding the current redistributor to node 6 over the southern branch of the network has been analyzed. For the northern branch, including nodes 1, 2 and 3, the impacts can be seen as well. Indeed, the oscillation of the control system of the current redistributor at node 6 influences the currents flowing from the main power supply to this node, inducing voltage variations on the path they take. The voltage balancer located at node 1 is maintaining the voltages of the poles equal at steady-state, but during the transient period the control system is not able to maintain this balance before it becomes stable. This unbalance at node 1 is propagating to nodes 2 and 3 in the same way it was propagating for the first scenario (Figure 4.2c). In this case, the unbalance levels are displayed in Figure 4.10.

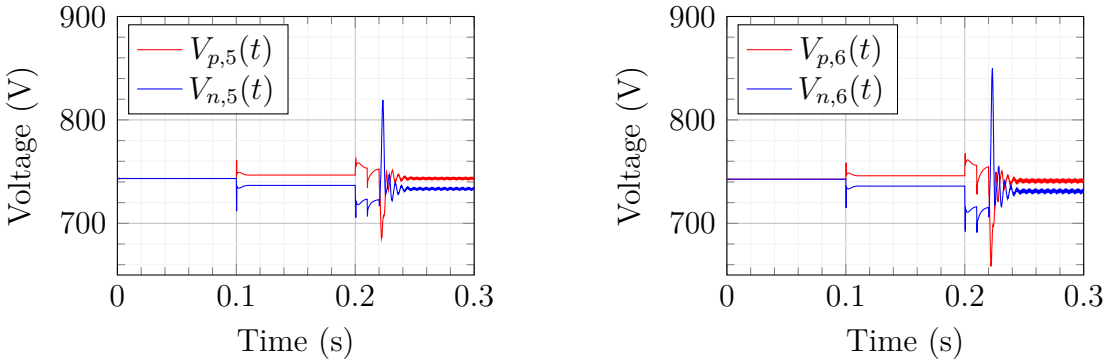

(a) Scenario 3 – Node 5 voltages

(b) Scenario 3 – Node 6 voltages

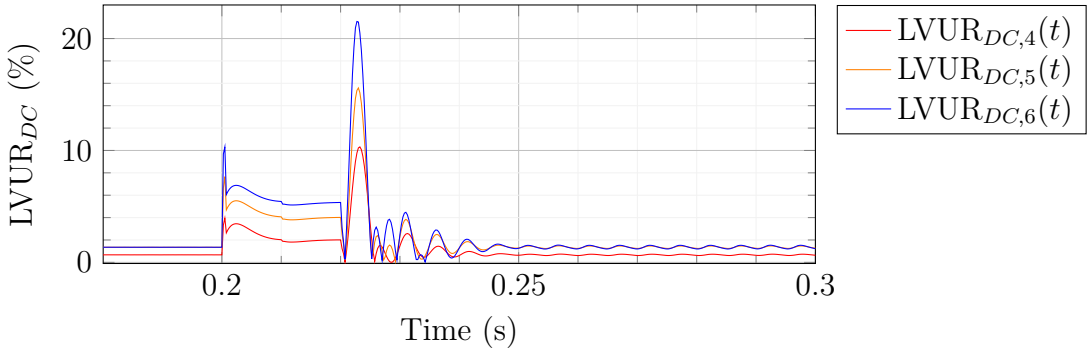

(c) Scenario 3 – Zoom on the LVUR_{DC} of node 4, 5 and 6

Figure 4.9: Scenario 3 – Comparison of the voltages of node 1 and node 6

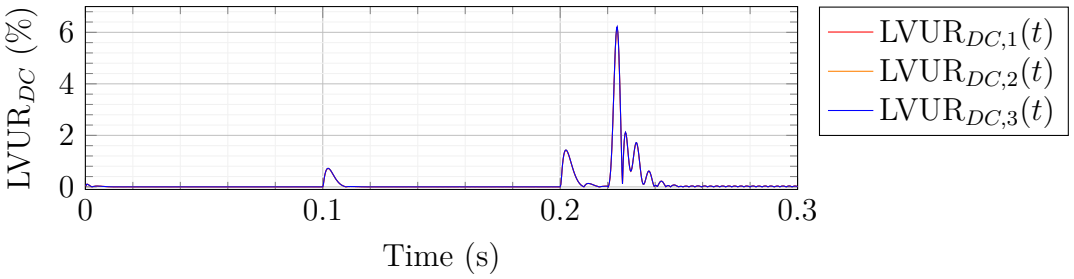

Figure 4.10: Scenario 3 – Comparaison of the LVUR_{DC} of nodes 1, 2 and 3

4.4 Fourth scenario

The fourth scenario is a combination of the second and the third one, including both the standalone voltage balancer at node 5 and the current redistributor at node 6. The goal of this simulation is to determine if it is possible to control both the currents and the voltages in a bipolar DC microgrid, and the impacts it might have on the surrounding nodes of the network.

First, one might expect the currents behavior at node 6 to be the same in this case and the third scenario. Indeed, the voltage balancer at node 5 has no impact on the currents at node 6. This was discussed in section 4.2 and is due to the fact that loads

are modeled as constant current loads.

Concerning the voltage levels on the other hand, the standalone voltage balancer at node 5 keeps the voltages of its poles balanced. Without the current redistributor at node 6 keeping the voltage drops on the poles equal, the line voltage unbalance rate would be non-zero at this node. When added, as seen in Figure 4.11, the voltages are kept balanced at node 6. This comes from section 1.3, stating that a voltage balancer and a current redistributor have the same impact on voltages and currents when they are placed downstream of a voltage balanced node.

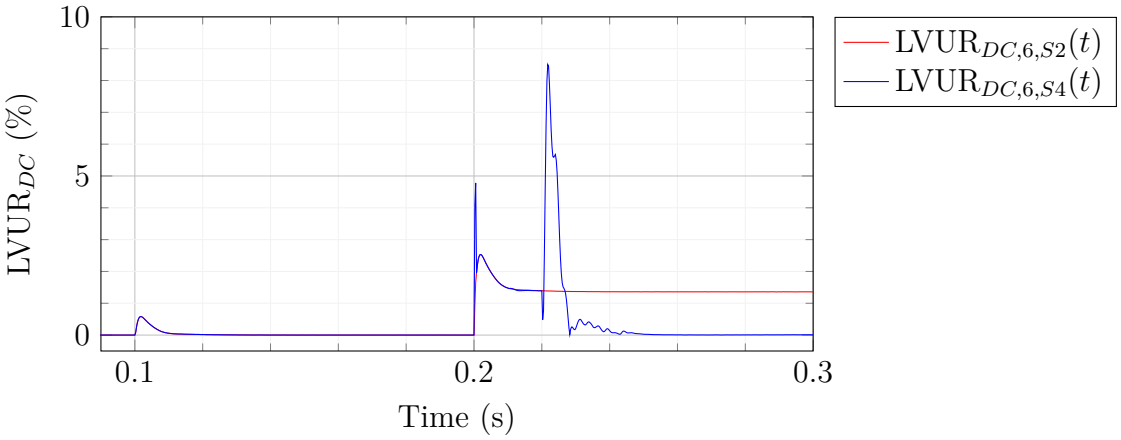

Figure 4.11: Comparison of LVUR$_{DC}$ at node 6 for the second (S2) and the fourth (S4) scenarios

The impact of adding a standalone voltage balancer upstream to the current redistributor of the third scenario can also be seen at node 1. Indeed, the voltage balancer at node 5 reduces the voltage deviations due to the transient of the current redistributor's control system. From the perspective of node 1, the LVUR$_{DC}$ goes from 6% to approximately 1.5%, or a reduction of 75% of this value, as displayed in Figure 4.12.

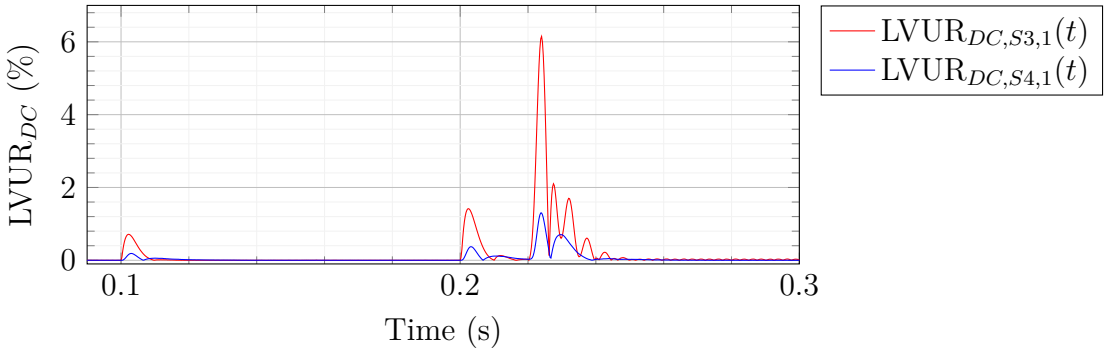

Figure 4.12: Comparison of LVUR$_{DC}$ at node 1 for the thirt (S3) and the fourth (S4) scenarios

4.5 Discussions

The discussion conducted in this chapter first focuses on the simulation results presented in the previous sections. Secondly, a brief overview of the current situation of bipolar DC microgrid standardization is given.

4.5.1 Simulation results

In summary, it can be observed that voltage balancing and current redistributing are two different controls that can be applied to a bipolar DC microgrid. This discussion suggests an answer to the last research question of this thesis, which is about how and where to position them in the network. Although the "how" part of the question was answered in chapter 2, the "where" depends on how the positioning of the devices affects the grid. This part of the question is discussed here.

First, the main voltage balancer is needed to create the bipolar DC microgrid's poles. It is the bridge between an unipolar network and a bipolar network. It also maintains voltage balance at this root node.

Even though the main voltage balancer keeps balance at the root node, uneven distribution of the loads might lead to voltage unbalances at some nodes and non-optimal currents distribution through some lines. Voltage unbalances at a node can lead to too high, or too low voltage for the connected loads. It can trigger security equipments, that can end up in loads getting disconnected or damaged. In that case, a standalone voltage balancer can be used, connected to a specific node in the microgrid. As seen in section 4.2, this device can keep the LVUR_{DC} equal to zero in steady-state. Its control system induces LVUR_{DC} variations during transient, which can be tuned. Indeed, the control system in this work is quite simple. It is possible to develop a more advanced control system that fits better the project's requirements.

The position of a voltage balancer can be determined by considering its two advantages. First, it can reduce voltage unbalance at its connection node, protecting sensitive loads from voltage deviations. Secondly, by maintaining voltage balance at some node in the grid, it prevents this unbalance to propagate to downstream power balanced nodes. In other words, a standalone voltage balancer can cancel upstream voltage unbalance's effect.

Regarding currents uneven distribution on the three wires due to uneven load powers on the poles, a current redistributor can be used. This device can maintain optimal current flows on a chosen line, limiting line losses.

An important aspect of using those two kinds of devices is to understand in what

ways they are alike or not. Indeed, as explained in section 1.3, a voltage balancer does not guarantee optimal currents distribution, and a current redistributor does not guarantee voltage balance. The only scenario in which they produce the same result is when they are placed just downstream of a voltage balanced node (meaning that the node's $\text{LVUR}_{DC} = 0$).

Moreover, when the grid's maintainer is a distinct entity from the owner of the loads, it is likely that their individual interests regarding each device may diverge. Indeed, whereas voltage balance is a problem for both of them, the current distribution problem affects them differently. From the loads standpoint, the current distribution over the lines does not change anything, as long as the voltages are kept to nominal values. On the contrary, additional losses on the lines can lead to higher costs and tears in the cables for the grid's owner.

4.5.2 Note on the current state of standardization for bipolar DC networks

To the author's best knowledge, there is no universally recognized standard specifically for bipolar DC networks. The International Electrotechnical Commission (IEC) technology report of 2017 [31] analyses and discusses the possibilities to use LVDC networks in complement of the already existing AC grids. LVDC networks have voltages going as high as 1500 V, hence the choice of 750 V per pole in the simulations. Another report of 2018 [36] critically reviews the international power quality standards IEEE Std1159 [37] and IEC 61000-4-30 [38] in the light of DC microgrid.

Both reports emphasize that standardization of voltages is a urgent key issue. By defining the voltages, it is also necessary to establish the criteria to consider for voltage selection. In [31], the chosen criteria is the power to be delivered. Once it is determined, it is then possible to select voltage and current levels, as well as the cable size, which makes it possible to have an usable implementation of this kind of network. Nevertheless, some power quality issues lead to voltage deviations and variations on the lines and need to be taken care of.

The IEEE Std1159 and IEC 61000-4-30 standards, developed for AC systems of 50Hz and 60Hz, might serve as base to develop unipolar and bipolar LVDC networks standards. Indeed, some concepts like transients, short- and long-duration variations and most waveform distortions are directly or close to directly usable for those types of electrical grids [36]. Besides this, EMC issues like AC offset (AC signal propagating on the DC voltage), voltage unbalance and current imbalance do not have clear definitions or indicators.

At the time of writing this thesis, the IEC is working on a standardization project for LVDC networks, encompassing both unipolar and bipolar configurations [39]. The proposal suggests treating bipolar DC networks as two separate unipolar DC networks. That way, it is possible to define standards solely for unipolar LVDC networks, and apply them to both poles of bipolar DC networks. In terms of power quality phenomena pertinent to LVDC networks, this committee draft represents one of the most advanced works available to date. It aims to define what power quality in LVDC networks is, and suggests nominal and maximum values for some of the considered power quality issues. However, it is not yet the case for voltage deviations.

Resulting from no universally recognized definitions for those values existing, no nominal ranges exist for them. It is then difficult to assess if the simulation results obtained in the previous section are good or not, because the definition of what would be acceptable values for the used indicators do not exist yet. Knowing those values are however crucial for any actors investing in the related technologies. As seen in chapter 2, for example, it is possible to size the components of the studied voltage balancers knowing the maximum voltage deviation allowed on the microgrid. The author of this thesis believes that without those standards made available and agreed on, it would slow down the deployment of such technology, keeping the potential investors back until the standards are clear and recognized on a large scale.

Chapter 5

Conclusion

This thesis aims to describe the problem of voltage unbalance that can occur in bipolar DC networks, and to suggest potential solutions to this problem.

A review of the literature was carried out as thoroughly as possible. From the literature review, potential solutions to the voltage unbalance problem were studied and analyzed according to several criteria like the dynamic response's speed or the number of components. This analysis served as knowledge base to choose three topologies that were used for the simulations. A detailed explanation about the design of the circuits of the solutions and their control system was given, in addition to a validation of their behaviors. A precharge circuit has been studied to be able to connect the balancing circuits to a network in operation. Once validated, those devices were used in a bigger testbench to show how their use impacts different nodes of the microgrid, and how they interact. From the obtained results, it was possible to give recommendations concerning the possible positions were voltage balancers and current redistributors should be connected, depending on their desired effects. Finally, the thesis concludes with a discussion about the current state of standardization for such electrical network, and how important it is to quickly have universally recognized standards.

It was eluded that unbalanced load conditions in the microgrid cause different currents to flow through the wires, leading to unequal voltage drops on the lines and ultimately to voltage unbalance. This issue has two main consequences. First, the voltage deviation resulting from this behavior might lead to over- or undervoltage, threatening loads disconnection because of their protection systems. This is a problem for the load's owner, but also for the grid operator that needs to make sure that the structure of the network itself can withstand those voltage deviations. Secondly, the imbalanced currents flowing through the wires lead to increased power losses on the cables. It was demonstrated that the line losses are at their minimum when the currents

in the positive and the negative wires are equal in magnitude, which is naturally the case with balanced load conditions. This issue is mainly a problem for the grid operator, increasing the potential maximum current and the conduction losses on the lines.

Although this problem constitutes a challenge for engineers designing such network, it is possible both to keep voltages balanced and currents optimally distributed in a bipolar DC microgrid. Indeed, the different voltage balancers and the current redistributor studied in this thesis showed to be effective. A power supply connected voltage balancer is able to trully create the bipolar DC network by introducing a neutral wire to the grid. A standalone voltage balancer can be used at any node of the network to cancel voltage unbalance at its connection point, and prevent its propagation to downstream nodes. Furthermore, making its connection node power balanced, a standalone voltage balancer can cancel voltage unbalance as seen by the upstream nodes. It thus has a positive action on both downstream and upstream parts of the grid. Finally, a current redistributor efficiently cancels the neutral wire's current, guaranteeing optimal line losses.

As most time and ressource limited research work, this thesis was made based on some assumptions and thus have some limitations, all presented in the most exhaustive manner in section 3.4.

Contribution to the field of Electrical Engineering

The lack of standards available for bipolar DC network shows that the technology is not yet ready to be used in real-life scenarios. Promisingly, research is showing growing interest for the subject since a decade. In this context, this thesis aims at being a knowledge base for anyone interested in building feasible projects of bipolar DC microgrid.

The comprehensive review of the different solutions to voltage unbalance and current imbalance, as well as their specific circuits, have been discussed. In addition to the data found in the literature, this report gives insight about different criteria that can help to make a choice from this pool of solutions. It also gives a detailled explanation of the design of such solutions. Finally, besides showing general results, this work goes further and analyzes the existing interactions between voltage balancers and current redistributors.

Future research

Although this thesis tries to be as complete and detailled as possible, there is still interesting ideas to explore. As listed in section 3.4, several aspects of the simulations can be improved and others scenarios considered.

It would be interesting to validate the simulations using a real testbench. By doing so, it would be possible to study its behavior with different kind of loads, going from purely resistive to ideal current sources, like discussed in this paper. It would also show the real behavior of the studied voltage balancers and current redistributor since they are modeled using ideal switches in Matlab / Simulink.

Moreover, integrating more power generation and energy storage systems would bring the studied cases closer to what a bipolar DC microgrid can aim to be: a localized network that facilitates the integration of renewable energy sources.

Additionally, whereas the control system of the voltage balancers seems robust, the current redistributor one is less optimal, showing bigger oscillations before operating stably. Several research papers suggest other controllers that the one discussed in this thesis, and fitting them to work with this device is believed to show better results.

Finally, investigating the balancing potential of loads, power sources and ESS with balancing capacities is thought to be a great way to conjunctly connect those elements to the grid, and to maintain voltage balance at their connection point.

Appendices

Appendix A: Isolated voltage balancer topologies

This appendix presents different topologies of isolated voltage balancer topologies. [1] provides good summary of existing solutions.

One solution to create a galvanic isolation is to use a dual-active bridge (DAB) converter, and then use a nonisolated voltage balancer like seen in subsection 1.5.1. The easiest one is represented in Figure 5.1a, which is a DAB followed by an interleaved half-bridge voltage balancer. This topology is composed of a high-frequency transformer creating the isolation, then a voltage balancing stage is added to create the neutral wire's voltage and thus obtain a bipolar architecture. A small variation and space optimization gives the topology of Figure 5.1b, which is the same as the previous one except that a power conversion stage has been removed, resulting in a better power efficiency.

If the voltages on the bipolar side of the transformer are considered too high for the switching devices, Figure 5.1c shows a triple-active bridge (TAB), which is essentially two DAB put on top of each other in the bipolar side, also known as DAB + DAB. The voltages supported by each switch is half of the total voltage. This advantage is obtained by approximately doubling the number of components, adding a three-winding transformer and a more complex control in order to obtain the voltage balance on the bipolar DC side. It is possible to keep this advantage of having half the total voltage supported by the switching devices with galvanic isolation without using a three-winding transformer. It is achieved by using three-level voltage balancers like seen in section 1.5.1. This architecture is illustrated in Figure 5.1d. The number of switching devices is the same, but a two-winding transformer is cheaper and tinier.

If for some application a galvanic isolation is required but the number of components has to stay low for some application specific reasons, it is possible to use a dual-active half-bridge (DAHB) as interface between the AC network and the high-frequency transformer. Figure 5.1e shows this DAHB in a voltage balancing circuit. Here, the

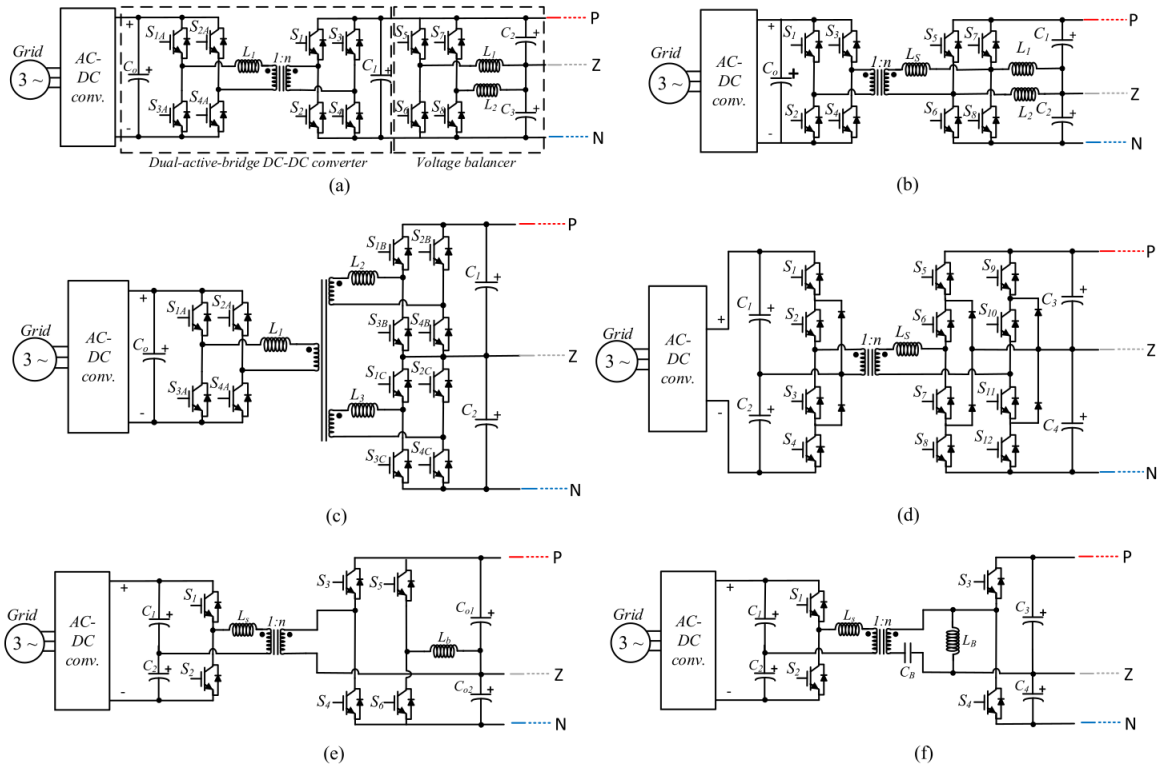

Figure 5.1: Summary of isolated source connected voltage balancers [1]

voltage balancing part is obtained using a very simple modified half-bridge voltage balancer. Following the same idea, Figure 5.1f shows one of the simplest implementation of galvanic isolation for bipolar DC voltage balancer [40]. It is composed of a DAHB and a Buck/Boost based voltage balancer. This solution suffer from less switching device's losses compared to the others.

Appendix B: Simulation testbench

Complete testbench

The complete implementation of the testbench used for the simulations is given in Figure 5.2. It corresponds to the Simulink model of the diagram in Figure 3.1. The details of the implementation for each parts of this model is explained in the following sections.

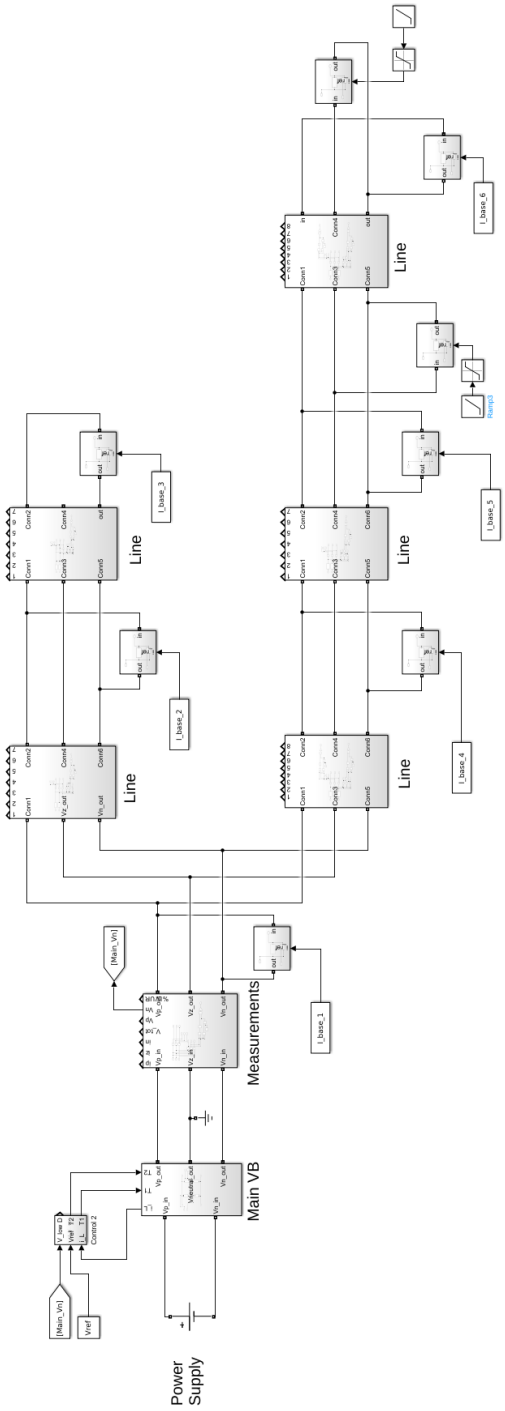

Figure 5.2: Full testbench implementation

Lines

The implementation of the lines used for the simulations is given in Figure 5.3. It consists of three parallel RL lines.

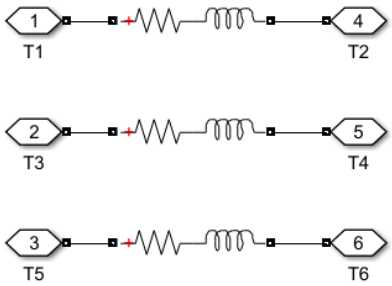

Figure 5.3: Simulink implementation of the lines

Main voltage balancer: unipolar-bipolar interface

The half-bridge voltage balancer is the interface between the unipolar and the bipolar sides of the microgrid. It creates the neutral wire's voltage by balancing dynamically the power distribution between the two poles. Its Simulink model implementation is given in Figure 5.4. The details of the design are given in chapter 2.

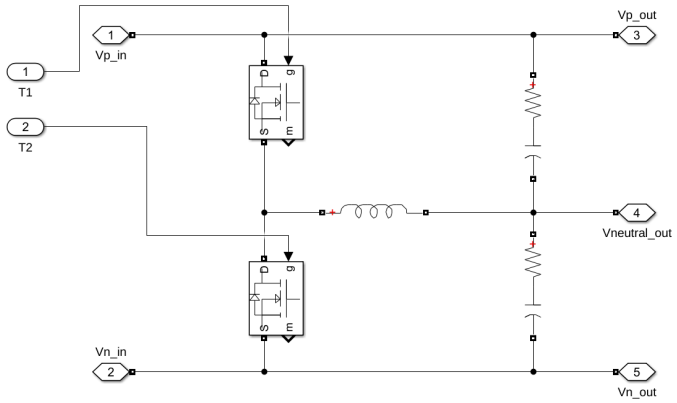

Figure 5.4: Simulink implementation of the main voltage balancer

Standalone voltage balancer

The Simulink implementation of the standalone half-bridge voltage balancer is given in Figure 5.5. The details of the design are given in chapter 2.

Current redistributor

The Simulink implementation of the current redistributor is given in Figure 5.6. The details of the design are given in chapter 2.

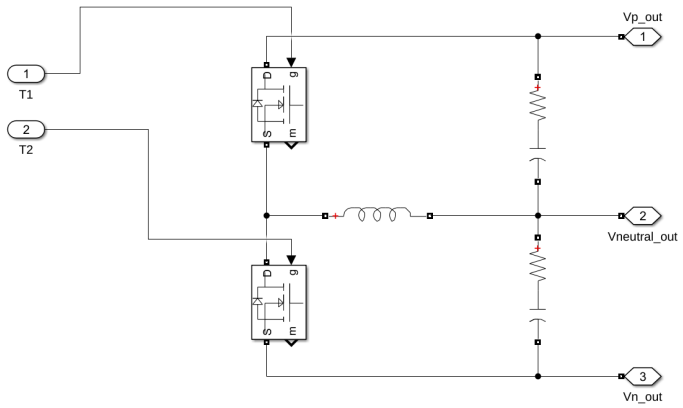

Figure 5.5: Simulink implementation of the standalone voltage balancer

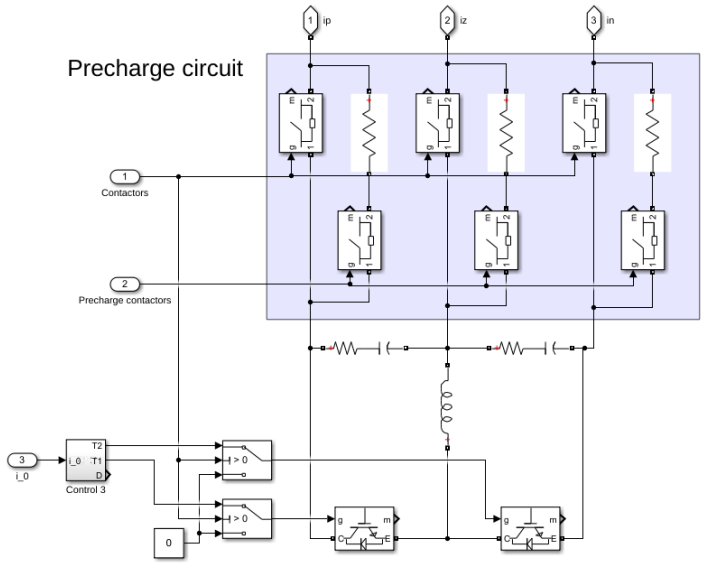

Figure 5.6: Simulink implementation of the current redistributor

Loads

The Simulink implementation of the current redistributor is given in Figure 5.7. The shunt resistor is added for the simulation software to be able to run the simulation. Its value is of $10^5\,\Omega$.

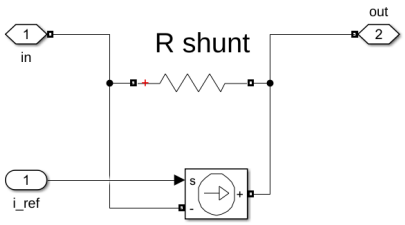

Figure 5.7: Simulink implementation of the loads

Appendix C: Power profiles of the loads

The power profiles are taken from data provided by a member of the research group with whom the author of this thesis is working. The actual values of the loads are not extremely important, the main goal is to have relatively realistic power curves to have a general idea of the magnitude of the powers involved in such a network. The data was simulated for the MIRaCCLE project [16]. This data is displayed in Figure 5.8. In order to see the total power drawn from the power supply, a cumulative graph is displayed in Figure 5.9.

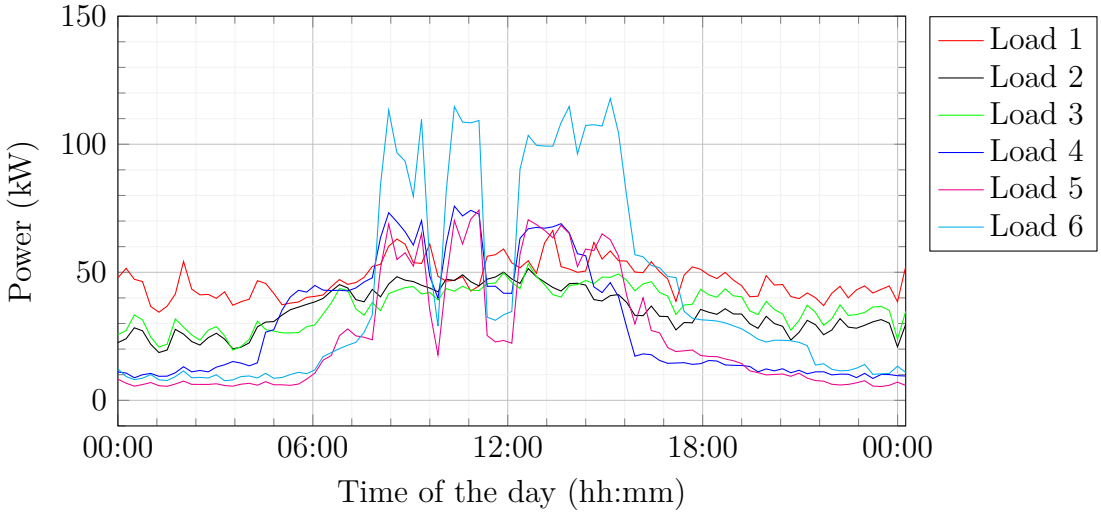

Figure 5.8: Simulated load profiles for the MIRaCCLE project

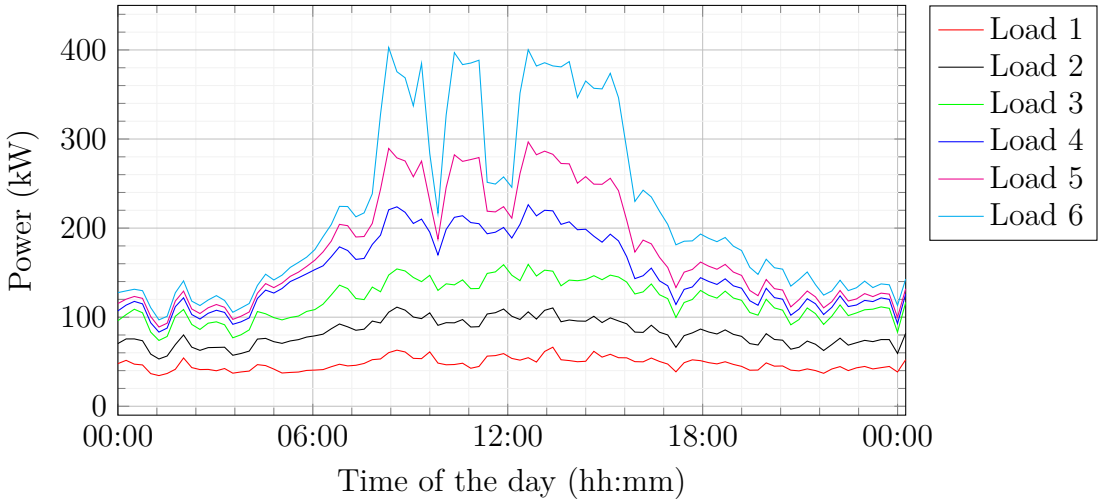

Figure 5.9: Simulated load profiles for the MIRaCCLE project – Cumulative

Bibliography

[1] V. F. Pires, A. Cordeiro, C. Roncero-Clemente, S. Rivera, and T. Dragicevic, "DC–DC Converters for Bipolar Microgrid Voltage Balancing: A Comprehensive Review of Architectures and Topologies," *IEEE Journal of Emerging and Selected Topics in Power Electronics*, vol. 11, pp. 981–998, Feb. 2023.

[2] F. Wang, Z. Lei, X. Xu, and X. Shu, "Topology Deduction and Analysis of Voltage Balancers for DC Microgrid," *IEEE Journal of Emerging and Selected Topics in Power Electronics*, vol. 5, pp. 672–680, June 2017.

[3] J. Lago, J. Moia, and M. L. Heldwein, "Evaluation of power converters to implement bipolar DC active distribution networks - DC-DC converters," in *2011 IEEE Energy Conversion Congress and Exposition*, (Phoenix, AZ, USA), pp. 985–990, IEEE, Sept. 2011.

[4] "Climate Change 2023 - Synthesis Report: Summary for Policymakers," tech. rep., Intergovernmental Panel on Climate Change (IPCC), 2023.

[5] "CO2 Emissions in 2022," tech. rep., International Energy Agency (IEA), Mar. 2023.

[6] "Renewable 2022: Analysis and forecast to 2027," tech. rep., International Energy Agency (IEA).

[7] C. Wu, X.-P. Zhang, and M. Sterling, "Solar power generation intermittency and aggregation," *Scientific Reports*, vol. 12, p. 1363, Jan. 2022.

[8] I. E. A. (IEA), "Offshore Wind Outlook 2019: World Energy Outlook Special Report," *Offshore Wind*, 2019.

[9] G. Ren, J. Liu, J. Wan, Y. Guo, and D. Yu, "Overview of wind power intermittency: Impacts, measurements, and mitigation solutions," *Applied Energy*, vol. 204, pp. 47–65, Oct. 2017.

[10] Zhang Jun-fang, Ding Si-min, Hang Yin-li, and Hu Guang, "Research on distributed generation source placement," in *2009 International Conference on Sustainable Power Generation and Supply*, (Nanjing), pp. 1–4, IEEE, Apr. 2009.

[11] Ding Xiaoqun, Wu Jiahong, and Zhao Feng, "Optimal location and capacity of distributed generation based on scenario probability," in *2009 International Conference on Sustainable Power Generation and Supply*, (Nanjing), pp. 1–5, IEEE, Apr. 2009.

[12] J. F. Manwell, "Chapter 5: Electrical Aspects of Wind Turbines," in *Wind Energy Explained: Theory, Design and Application*, pp. 205–256.

[13] D. Kumar, F. Zare, and A. Ghosh, "DC Microgrid Technology: System Architectures, AC Grid Interfaces, Grounding Schemes, Power Quality, Communication Networks, Applications, and Standardizations Aspects," *IEEE Access*, vol. 5, pp. 12230–12256, 2017.

[14] "What are Microgrids and Why are They Becoming So Popular?." `https://enchantedrock.com/what-are-microgrids/`. (accessed 2023-05-23).

[15] N.-K. Hong, J.-W. Park, S.-J. Chung, C.-H. Noh, S.-H. Sohn, G.-H. Gwon, and C. H. Kim, "Analysis of Load Unbalance According to Topology of Bipolar Low Voltage DC Distribution System," in *TENCON 2018 - 2018 IEEE Region 10 Conference*, (Jeju, Korea (South)), pp. 0747–0751, IEEE, Oct. 2018.

[16] "MIRaCCLE – Klinkenberg S.A.." `https://klinkenberg.be/miraccle/`. (accessed 2023-05-23).

[17] S. D. Tavakoli, M. Mahdavyfakhr, M. Hamzeh, K. Sheshyekani, and E. Afjei, "A unified control strategy for power sharing and voltage balancing in bipolar DC microgrids," *Sustainable Energy, Grids and Networks*, vol. 11, pp. 58–68, Sept. 2017.

[18] S. Rivera, R. Lizana F., S. Kouro, T. Dragicevic, and B. Wu, "Bipolar DC Power Conversion: State-of-the-Art and Emerging Technologies," *IEEE Journal of Emerging and Selected Topics in Power Electronics*, vol. 9, pp. 1192–1204, Apr. 2021.

[19] C. Zhang, D. Jiang, H. Zheng, and L. Ye, "A Bi-Directional Buck/Boost Voltage Balancer for DC Distribution System," in *2013 Fourth International Conference on Digital Manufacturing & Automation*, (Shinan District of Qingdao ¿Shangdong Province, China), pp. 9–13, IEEE, June 2013.

[20] X. Zhang, C. Gong, and Z. Yao, "Three-Level DC Converter for Balancing DC 800-V Voltage," *IEEE Transactions on Power Electronics*, vol. 30, pp. 3499–3507, July 2015.

[21] J.-M. Park, T.-H. Park, B.-J. Kim, K.-M. Choo, and C.-Y. Won, "The Interleaved Buck/Boost Type Voltage Balancer with Coupled-inductor in Bi-polar DC Microgrid," in *2019 IEEE Transportation Electrification Conference and Expo, Asia-Pacific (ITEC Asia-Pacific)*, (Seogwipo-si, Korea (South)), pp. 1–5, IEEE, May 2019.

[22] P. Prabhakaran and V. Agarwal, "Mitigation of voltage unbalance in a low voltage bipolar DC microgrid using a boost-SEPIC type interleaved dc-dc compensator," in *2016 IEEE 2nd Annual Southern Power Electronics Conference (SPEC)*, (Auckland, New Zealand), pp. 1–6, IEEE, Dec. 2016.

[23] H. Kakigano, Y. Miura, and T. Ise, "Low-Voltage Bipolar-Type DC Microgrid for Super High Quality Distribution," *IEEE Transactions on Power Electronics*, vol. 25, pp. 3066–3075, Dec. 2010.

[24] H. Kakigano, Y. Miura, T. Ise, and R. Uchida, "DC Voltage Control of the DC Micro-grid for Super High Quality Distribution," in *2007 Power Conversion Conference - Nagoya*, (Nagoya, Japan), pp. 518–525, IEEE, Apr. 2007.

[25] J.-Y. Kim, H.-S. Kim, J.-W. Baek, and D.-K. Jeong, "Analysis of Effective Three-Level Neutral Point Clamped Converter System for the Bipolar LVDC Distribution," *Electronics*, vol. 8, p. 691, June 2019.

[26] "Why Do We Need Galvanic Isolation? - FAQS Clear." `https://www.faqsclear.com/why-do-we-need-galvanic-isolation/`, May 2022. (accessed 2023-03-27).

[27] T. D. Mai, T. Verschelde, and J. Driesen, "Comparative study of current redistributor's topologies for mitigating unbalanced currents in bipolar DC microgrids," in *2017 IEEE Second International Conference on DC Microgrids (ICDCM)*, (Nuremburg), pp. 242–247, IEEE, June 2017.

[28] M. Bekemans, "LELEC2660 - Power Electronics: 2. DC-DC Converter," Mar. 2022.

[29] R. W. Erickson and D. Maksimović, "7.3 Modeling the Pulse-Width Modulator," in *Fundamentals of Power Electronics*, pp. 242–245, Cham, Switzerland: Springer International Publishing, 2020.

[30] R. W. Erickson and D. Maksimović, "18.9 Average Current-Mode Control," in *Fundamentals of Power Electronics*, pp. 786–797, Cham, Switzerland: Springer International Publishing, 2020.

[31] IEC, "LVDC: Electricity for the 21st century," tech. rep., 2017.

[32] B. INC., "IGBT vs MOSFET - Determining the Most Efficient power Switching Solution," Aug. 2022.

[33] C. Chang and T. Chen, "Why Pre-Charge Circuits Are Necessary in High Voltage Systems," 2021.

[34] A. Von Jouanne and B. Banerjee, "Assessment of voltage unbalance," *IEEE Transactions on Power Delivery*, vol. 16, no. 4, pp. 782–790, Oct./2001.

[35] N. E. M. Association, "AMERICAN NATIONAL STANDARD for Electric Power Systems and Equipment - Voltage Ratings (60 Hertz)," Tech. Rep. C84.1, 1995.

[36] G. Van Den Broeck, J. Stuyts, and J. Driesen, "A critical review of power quality standards and definitions applied to DC microgrids," *Applied Energy*, vol. 229, pp. 281–288, Nov. 2018.

[37] "IEEE Recommended Practice for Monitoring Electric Power Quality," pp. 1–94, 2009.

[38] "Electromagnetic compatibility (EMC) - Part 61000-4-30: Testing and measurement techniques - ower quality measurement methods," tech. rep., International Electrotechnical Commission (IEC), Mar. 2021.

[39] "IEC TR 63282 ED2," Tech. Rep. 8/1655/CD, International Electrotechnical Commission (IEC), 24th of April 2023.

[40] K. Kim and H. Cha, "Dual-Active-Half-Bridge Converter With Output Voltage Balancing Scheme for Bipolar DC Distribution System," *IEEE Transactions on Industrial Electronics*, vol. 69, pp. 6850–6858, July 2022.

UNIVERSITÉ CATHOLIQUE DE LOUVAIN
École polytechnique de Louvain
Rue Archimède, 1 bte L6.11.01, 1348 Louvain-la-Neuve, Belgique | **www.uclouvain.be/epl**